Space Shift Keying in the Presence of Multiple Co-Channel Interferers

by
Guriqbal Singh

A Thesis
Presented to Lakehead University
in Partial Fulfillment of the Requirement for the Degree of
Master of Science
in
Electrical and Computer Engineering

Thunder Bay, Ontario, Canada

September, 2016

Abstract

Guriqbal Singh. Space Shift Keying Modulation in the Presence of Multiple Co-Channel Interferers (Under the Supervision of Dr. Salama Ikki).

In this thesis, the performance of Space Shift Keying (SSK) Modulation, a technique for Multiple Input Multiple Output (MIMO) wireless communication systems is studied. The results are analyzed and compared assuming absence as well as presence of Co-Channel Interference (CCI).

SSK Modulation is based on the concept of Spatial Modulation (SM) technique for MIMO systems. In SM, only one transmitting antenna remains in the state of action at a single point in time while others remain in sleep mode, resulting in no Inter Channel Interference (ICI). This is another reason for the increase in system performance and spectral efficiency.

Unlike SM, in SSK Modulation there is no transmission of data symbols. However, the index of transmitting antenna is transmitted, resulting in advantages such as a reduction in detection complexity and hardware cost as there is no need for Amplitude Phase Modulation (APM) elements at both transmitting and receiving end.

In this work, the exact analytical expression for Average Bit Error Rate (ABER) of SSK Modulation in the presence of CCI has been derived, and the same is further supported by MATLAB simulated results. The analysis with CCI is necessary because the spectral efficiency of the communication system can be improved by a reduction in the re-use factor of the co-channel; however, reducing the re-use factor also raises the co-channel interference.

Performance for the systems with single as well as multiple receiving antennas has been analyzed twice considering correlated and uncorrelated Rayleigh fading channels. The asymptotic analysis results for uncorrelated Rayleigh fading channels have also been derived and compared with exact results.

Acknowledgments

First and foremost, my deepest appreciation goes to my supervisor - professor, Dr. Salama S. Ikki (Faculty, Department of Electrical Engineering, Lakehead University). Dr. Ikki has continually supported me and helped me in every step of the way. He gave me the motivation and the spirit to help me achieve my goals. Without his guidance, I could not have completed this research.

I would also like to thank Mr. Raman Trivedi (DGM-R&D MicroMet-ATI Pvt. Ltd.) and Dr. Eylem Erdogan. I am extremely grateful for their expertise, guidance and their encouragement which they have given.

Furthermore, my special gratitude goes to the review committee, Dr. Ali Afana and Dr. Dimiter Alexandrov for their feedback and approval of this research.

In addition, I would like to acknowledge my close friends; Simardeep Singh Gill and Kanwarbir Singh Bajwa. During my research, I was able to get feedback and advice on my research techniques or report writing. For motivation and support, I would like to recognize Jaspreet Kaur Khela.

Moreover, I also thank my mother as she helped me on every step of my journey. Also, with heavenly blessings of my father, I was able to complete this research.

Finally, I would like to sincerely thank all the faculty members of the Department of Electrical Engineering at Lakehead University for their encouragement and help. I also would like to extend my gratitude to all who helped me in one way or another.

Guriqbal Singh

gsingh9@lakeheadu.ca

Contents

List of Figures

List of Tables

List of Abbreviations

MIMO	–	Multiple Input Multiple Output.
SISO	–	Single Input Single Output.
ZF	–	Zero Forcing
SIMO	–	Single Input Single Output
MISO	–	Multiple Input Single Output
MRC	–	Maximul Ratio Combining
ML	–	Maximum Likelihood
VBLAST	–	Vertical Bell Laboratories Space Time
SMX	–	Spatial Multiplexing
SM	–	Spatial Modulation
SSK	–	Space Shift Keying
BPSK	–	Binary Phase Shift Keying
SNR	–	Signal to Noise Ratio
HYB	–	Hybrid
DIV	–	Diversity
BER	–	Bit Error Rate
BEP	–	Bit Error Probability
SER	–	Symbol Error Rate
SEP	–	Symbol Error Probability
ABER	–	Average Bit Eror Rate
ABEP	–	Average Bit Error Probability
AABER	–	Asymptotic Average Bit Error Rate
CBER	–	Conditional Bit Error Rate
CCI	–	Co-Channel Interference
PDF	–	Probability Density Function

Chapter 1

Introduction

1.1 Wireless Communication and Communication Systems

Wireless communication is one of the biggest gifts to mankind among technologies. Based on the survey conducted by Statista, the number of users were exponentially increased from 4.01 billion to 4.43 billion over the years from 2013 to 2015, and are further expected to increase up to 4.77 billion in 2017 [1]. The number of users and cellular data traffic are interdependent where data traffic and the number of users are proportional. The increase in data traffic can be explained because the users are extensively using e-books, Android/ Apple applications such as social networking, video streaming, emails etc. Due to this increase of data traffic, mobile operators are struggling to satisfy the users with a faster data rate [2].

Depending upon the number of antennas (antenna configuration) at the transmitting and receiving ends, communication systems are divided into four categories: the single input single output (SISO) systems, single input multiple output (SIMO) systems, multiple input single output (MISO) systems, and multiple input multiple output (MIMO) systems. In SISO systems, a single antenna is used at both transmitting and the receiving ends as shown in Fig. 1.1. In SIMO systems, there is only one antenna at the transmitting end and multiple antennas at the receiving end as shown in Fig. 1.2. In MISO systems, as shown in Fig. 1.3, there are multiple antennas at the transmitting end but only one antenna at the receiving end. However, in MIMO systems, as shown in Fig. 1.4., there are multiple antennas at both the transmitting as well as

the receiving ends.

Even though wireless communication provides countless benefits such as satellite communications or driver-less vehicles, there are many challenges to overcome. Each wireless system suffers from the problems of the reliability of transmitted information, high-speed data transfer or data rate and high spectral efficiency. Other problems include optimal data detection technique with low complexity at low-cost [3], power-efficient data processing, signal fading, Co-Channel Interference (CCI), and restricted availability of frequency spectrum.

It was shown that MIMO systems are an efficient solution to the above challenges by Foschini et al. [4–6]. This study concluded that the asymptotic capacity of systems with multiple antennas at the transmitting and receiving ends are linearly proportional to the transmitting antennas under the effect of Rayleigh fading channels.

The multiple element antenna array set up in the MIMO system results in the capacity of the system to be increased linearly with the increase in the number of antennas [3]. If the performance of MIMO systems is compared with the performance of SISO systems, MIMO systems offer high reliability of data transfer along with higher data rate [7]. For MIMO systems with a small number of transmitting and receiving antennas, there was a linear increase in information-theoretic capacity observed in scattering environments, at a high SNR (Signal to Noise Ratio) [8]. MIMO works on the principle of multiplexing multiple data symbols in space and transmitting them without an increase in bandwidth. MIMO systems also reduce the effect of multi-path fading. MIMO systems can be exploited in different ways to achieve the multiplexing gain of an antenna array, but this is achieved at the cost of high complexity and at a high cost of implementation [9]. MIMO systems are divided mainly into three sections: spatial multiplexing, diversity transmission, and hybrid transmission.

In spatial multiplexing, multiple antenna arrays are used at the transmitting end to transmit more information at a time. Vertical Bell Laboratory Layered Space Time (V-BLAST) is an

Figure 1.1: Single Input Single Output System

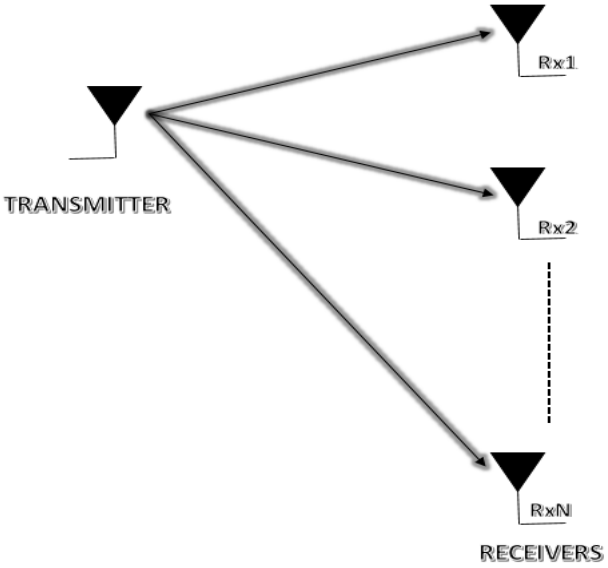

Figure 1.2: Single Input Multiple Output System

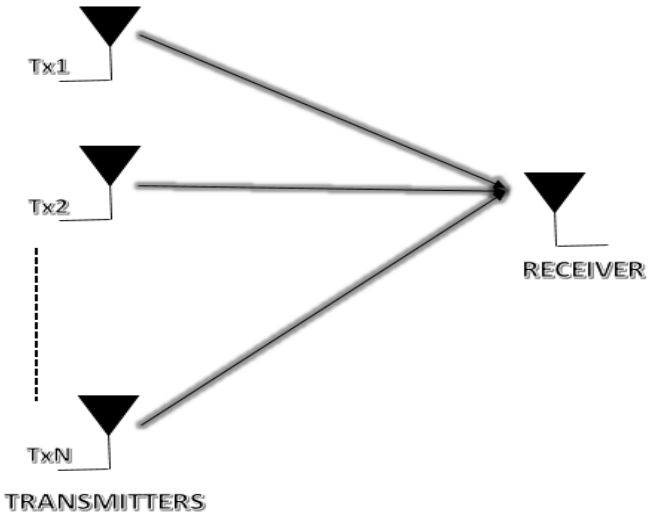

Figure 1.3: Multiple Input Single Output System

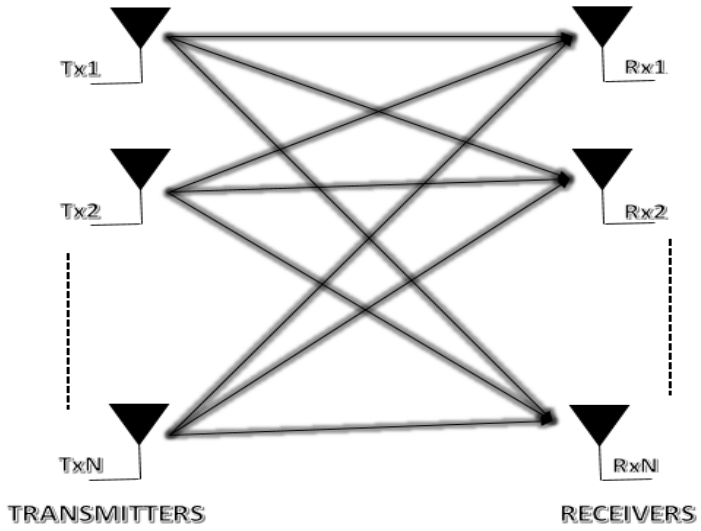

Figure 1.4: Multiple Input Multiple Output System

example of spatial multiplexing. V-BLAST is a layered structured data detection algorithm proposed by Bell laboratories to exploit high spectral capacity offered by MIMO channels [4, 10]. In V-BLAST, multiple data symbols are multiplexed and transmitted at the same time over all the channels without the need of an increase in bandwidth. At the detector location, data streams are separated and detected using an interference elimination and combination of array processing techniques.

In diversity transmission, multiple antennas are used to increase the reliability of information. Alamouti scheme is an example of diversity transmission [11], in which two transmitting antennas are used in order to obtain diversity at the transmitting end. The drawback of increasing the system diversity is that with the increase in diversity there is a decrease in spectral efficiency, which does not change in SIMO systems [12]. Researchers have overcome this problem by adding a third section to the MIMO systems, which is named hybrid multiple input multiple output (HYB MIMO) systems.

HYB MIMO system is the combination of both a spatial multiplexing technique and a diversity transmission technique. HYB MIMO system is a multi-layered space-time coding system

that provides diversity gain along with the increase in spectral efficiency [13].

1.2 Spatial Modulation Technique for MIMO Systems

SM is one of the MIMO system techniques in which SSK is used along with the amplitude phase modulation to transfer data symbols over the MIMO channels [14]. SM and SSK entirely avoids Inter Channel Interference and attains high Spectral efficiency at low system complexity and low implementation cost, without requiring antenna synchronization at transmitting end [9, 15].

Using a SM technique, Spectral efficiency shows a rise by logarithm to the base two of the number of transmitting antennas ($log_2 N_t$, where N_t is the number of transmitting antennas) as compared to SISO system [16]. If compared with other MIMO techniques like Vertical Bell Laboratory Layered Space-Time and Space-time Coding (STC), SM has higher error performance with a moderate number of transmitting antennas [17].

In SM, the information is modulated by activating a single transmitting antenna at a time (i.e. in each time slot) while keeping other transmitting antennas in a sleep state, which results in the elimination of inter-channel interference along with the achievement of high multiplexing gain [9, 18]. As only one antenna is being used at a single point in time, this requires only one Radio Frequency (RF) chain, which reduces the hardware cost and signal processing power of the system [16]. Activating a single antenna at each time reduces the complexity of the system without reducing data rate and system performance [18]. Also, in SM there is no requirement for time synchronization between antennas [15, 19].

In SM, information data are mapped with an antenna index of the active transmitting antenna to be used for transmission [9]. In SM, the receiver part is designed using a Maximum Likelihood (ML) detection technique for the estimation of transmitted data as well as the index of active transmitting antenna from which the received data were transmitted [20]. The ML detector is considered as an optimal detector for MIMO systems to minimize the Average Error

Probability(AEP) [21].

ML detector offers very low complexity and works on the principle of minimizing the Euclidean distance to the receive vector [22]. ML detector performs a search operation on all the received combinations of data and selects the best-related data. As in SM, there is activation of one antenna at a single point in time, so the complexity of the ML detector decreases as compared to the complexity of other detection techniques used in MIMO systems. For MIMO SM the complexity of the ML detector is shown to be identical to the complexity for SIMO system.

SM is shown to be a better technique for implementation in large MIMO systems [23–26]. The high increase in data traffic has focused researchers on using a large number of antennas; i.e.; tens to hundreds of antennas at both transmitting and receiving ends. This technique is termed Large MIMO or Massive MIMO; [27–31] shows the growth in data rate and improved Bit Error Rate (BER) performance of large MIMO systems.

1.3 Problem Statement, Relevant Works and Motivation

There are several types of digital communication systems, but almost each of the communication system needs a physical channel to transmit data, and these physical channels are not only subjected to noise but also to fading. Multi-path fading is commonly observed in wireless communication systems, which occurs because of constructive and destructive multi-paths received with delays and attenuation. Rayleigh distribution is one of the very common multi-path fading models with no line of sight.

Besides fading, Inter User Interference (Interference from other users) plays an important role to degrade the performance of wireless systems. Wireless signals are more severely subjected to Interference because of more base stations and mobile users. One of the main kinds of interference is Co-channel Interference (CCI), which is produced due to the frequency re-use.

Many researchers have studied and analyzed the performance of SSK, SM in the presence

of different types of fading channels with perfect/ imperfect Channel State Information(CSI) or channel estimation. The works in [26, 33, 39] showed that the performance of SSK is better than many other conventional techniques of modulation.

By computing the Outage error probability and Shannon capacity of SM in the presence of Rayleigh fading channels, M. M Ulla Faiz et al. in [34] have developed an information theoretic framework. When compared to space-time block coding, the framework shows that SM provides the increase in capacity on increasing the number of transmitting antennas.

The authors in [19, 32, 35], have studied the Average Bit Error Probability (ABEP) for SM in a presence of Rayleigh fading channels. Researchers have analyzed Symbol Error Probability of SM for a suboptimal receiver in [19] and have clearly shown that, as compared to V- BLAST and Alamouti scheme, SM provides better performance along with low detection complexity and the same spectral efficiency. In [32], the authors have derived closed form expression for ABEP for SM using optimal detection technique at the receiver. In [35], the authors derived the upper bound closed form expression for ABER of SM in the presence of correlated Rayleigh fading channel.

The authors of [12] have provided detailed analysis for the performance of coded-SSK and have derived closed form upper bound expression for Bit Error Probability (BEP) of SSK. The authors have observed that SSK provides gain over the Amplitude Pulse Modulation (APM), demonstrating that coded-SSK provides more capacity over APM.

In the presence of correlated Rician fading channels, the performance of SK has been analyzed in [36]. Marco Di Renzo et. al. in [36] proposed a general framework for the calculation of ABEP, considering the random number of receiving antennas and two transmitting antennas in the presence of arbitrary independent co-relation and channel coefficients of Rician fading channels. In [37] and [38], the authors have derived closed form exact and asymptotic upper bound expressions for ABER of SM, SSK in the presence of correlated Nakagami-m fading channels.

In all of the above-mentioned studies, the perfect CSI is considered whereas in [39] and [40], the authors have assumed imperfect CSI at receiver. In [39], Salama S. Ikki et al. have obtained an exact closed form and asymptotic expressions for ABEP of SSK, using the ML detection technique at receiver, in the presence of Rayleigh fading channels. In [40], the authors have studied through Monte Carlo simulations, and have shown that as compared to other techniques, SM is more robust to channel estimation error.

These works have improved an understanding of SSK. Motivated by the various benefits of using SSK and SM for MIMO systems and recent works on SSK have pushed an interest to analyze the performance of SSK in the presence of CCI. To study the effect of CCI is of major importance because spectral efficiency can be raised by decreasing the re-use factor of the co-channel but this also raises CCI [41].

1.4 Thesis Contribution

1. In this thesis, exact expressions for ABER have been derived using ML detection technique and the performance of SSK in the presence of multiple co-channel interferers has been analyzed for a system with a single receiving antenna. The results are derived and analyzed, assuming that the perfect CSI is available. The exact expression of ABER has been derived for two cases, a) when the fading channels are uncorrelated, and b) when the fading channels are correlated. In this thesis, ABER is used as a performance parameter to analyze the performance of system because its is considered as the most enlightening illustrator of the performance of the system. ABER can be derived by averaging Conditional Bit Error Rate (CBER) over fading statistics. The expression of asymptotic ABER has also been derived, as this gives insight into the performance of the system at high Signal to Noise Ratio (SNR). Furthermore, the mathematically derived results have also been verified by comparing with simulations developed in MATLAB.

2. The exact and asymptotic expressions of ABER have been generalized for the system with an arbitrary number of multiple receiving antennas using Maximum Ratio Combining (MRC) based ML detector. MRC is an optimal receiver diversity combining technique for noise limited systems. MRC improves the reliability and performance of transmission in flat fading channels. In MRC, each received signal after being multiplied with weight, is linearly added to another. The weights are chosen in such a way that the output SNR of the combiner or adder should be maximum (weights are the conjugate of fading channel coefficients) [46, 47]. When the power of the noise at all antennas is the same, the weight vector is the desired user's channel vector. Throughout the analysis in this thesis, the same noise power at all the branches is assumed. Moreover, the mathematically derived results have also been compared with MATLAB simulations in order to justify the accuracy of results.

1.5 Thesis Outline

The rest of thesis has been organized as follows:

In Chapter 2, two system models of SSK have been analyzed. Firstly, the system model with two antennas at transmitting end and one antenna at receiving end is studied. Secondly, the system model with two transmitting and an arbitrary number of N_r (multiple) receiving antennas is studied. For both the systems, mathematically derived exact analytical expressions for ABER in the absence of CCI are provided, assuming two different conditions. In the first condition, zero correlation in fading channels (uncorrelated fading channels) is assumed and in the second condition, correlated fading channels are assumed. Moreover, MATLAB based simulation results are provided in order to support the accuracy of theoretical results. In this chapter, asymptotic analysis has also been provided for both the system models.

In Chapter 3, the detailed mathematical analysis has been provided to calculate the exact expressions of ABER for both systems mentioned in Chapter 2, with and without correlation in fading channels. Also, the asymptotic ABER expressions for both the systems are derived.

Whereas in chapter 2 no CCI is assumed, in Chapter 3, it is assumed that the receiving antennas are subjected to Gaussian CCI. In this chapter also, the MATLAB simulation results are provided to justify the accuracy of theoretical results.

In Chapter4, the conclusion is stated and the future applications of SSK Modulation are highlighted.

Chapter 2

Space Shift Keying Modulation

SM was introduced by R. Mesleh [15, 19] with the intention to avoid inter channel interference (ICI), to get rid of inter-antenna synchronization(IAS), to reduce system complexity, to enhance spectral efficiency of MIMO systems as compared to the other MIMO techniques.

SSK Modulation is the special case of SM, in which only the antenna indices are transmitted to relay the information; the data symbols are not transmitted. As in SSK Modulation data symbols are not transmitted; therefore, there is no need of transceiver elements for the transmission and detection of APM (Amplitude/Phase Modulation). As compared to SM, SSK offers less detection complexity.

2.1 System Model

2.1.1 Single Receiving Antenna

Shown in Fig. 2.1 and 2.2 is the first system, where two transmitting antennas and the single receiving antenna are considered. In SSK, only one transmitting antenna is in a state of action at a single point in time, resulting in the need for only one RF chain. Fig. 2.1 refers to the time instance when 0 is the data to be transmitted; therefore, transmitting antenna Tx1 is in active mode and Tx2 is in sleep mode. Similarly, Fig. 2.2 shows the time instance when 1 is the data to be transmitted; thus, transmitting antenna Tx2 is in active mode and Tx1 is in sleep mode.

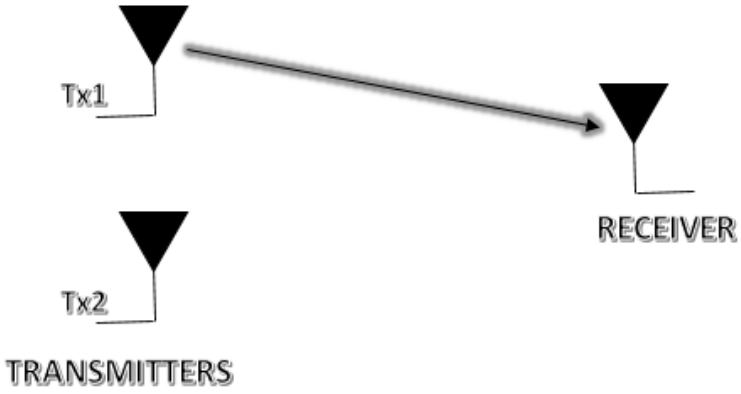

Figure 2.1: When transmitting data= 0, single receiving antenna

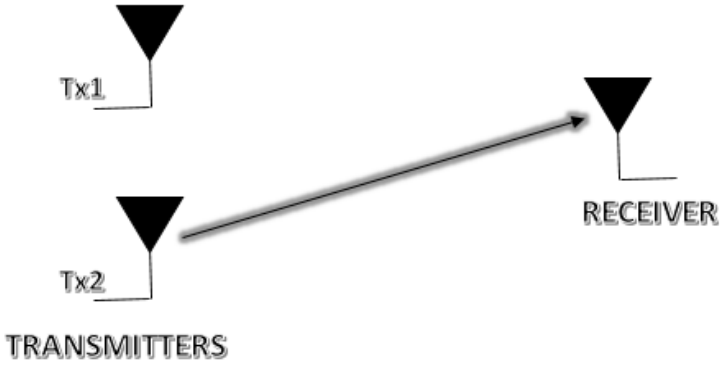

Figure 2.2: When transmitting data= 1, single receiving antenna

2.1.2 Multiple Receiving Antennas

Figures 2.3 and 2.4 show the second system, where two transmitting antennas and N_r (multiple) receiving antennas are considered. In this system, MRC is used as the diversity combining scheme. Figures 2.3 and 2.4 give an idea of the working of transmitting antennas. Fig. 2.3 tells about the system when 0 is the data to be transmitted, which causes the activation of transmitting antenna Tx1 and deactivation of Tx2; therefore, Tx 1 is sending data to all the receiving antennas. Similarly, Fig. 2.4 shows the system at a time when transmitting antenna Tx2 is in active mode and Tx1 is in sleep mode; this happens when 1 is the data to be transmitted.

2.2 System Model for Simulation

2.2.1 Single Receiving Antenna

Figure 2.5 shows the system model with single receiving antenna developed for the simulations in MATLAB.

2.2.2 Multiple Receiving Antennas

Figure 2.6 shows the system model with multiple receiving antennas developed for the simulations in MATLAB.

2.3 Performance Analysis for Single Receiving Antenna with Perfect CSI and no Co-channel Interferer

2.3.1 Exact Analysis in Presence of Uncorrelated Rayleigh Fading Channels

Transmission and Reception

The received signal at the receiving end can be written as

$$y = \sqrt{E} h_j + n, \qquad j = 1, 2, \tag{2.1}$$

where, $\sqrt{E}$ is the energy of desired signal, h_j is the complex Gaussian Rayleigh fading channel of activated transmitting antenna with mean zero and variance 1, $h_j \sim \mathcal{CN}\ (0, 1)$ and n is the complex Gaussian white noise with mean 0 and variance N_0, $n \sim \mathcal{CN}\ (0, N_0)$.

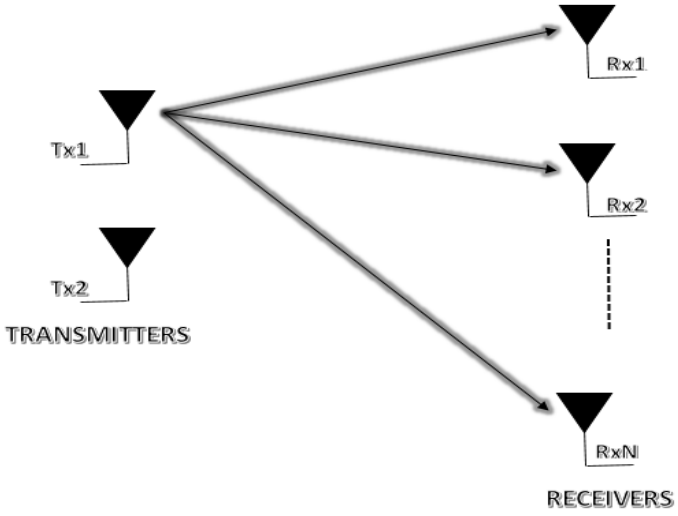

Figure 2.3: When transmitting data= 0, Multiple receiving antennas

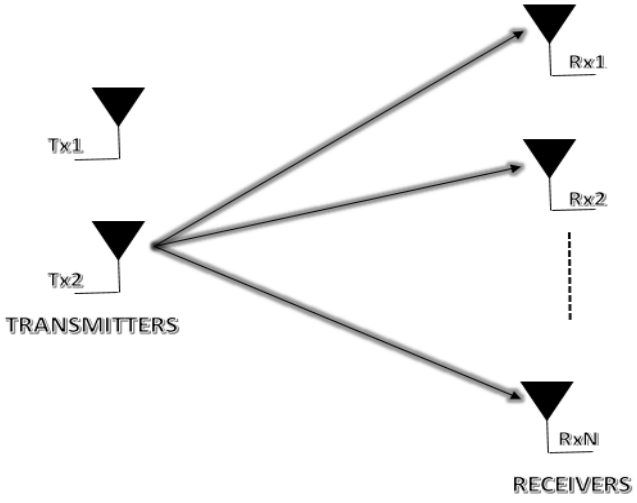

Figure 2.4: When transmitting data= 1, Multiple receiving antennas

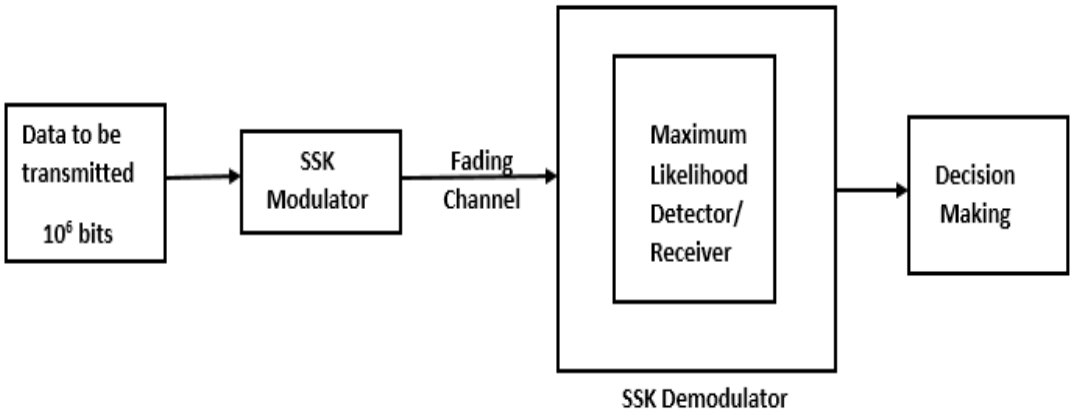

Figure 2.5: Block diagram of system with single receiving antenna used for simulation

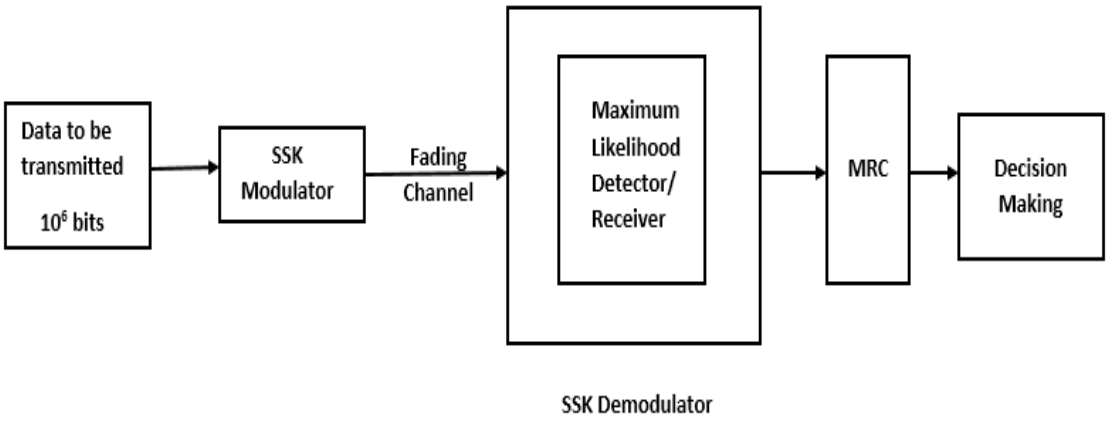

Figure 2.6: Block diagram of system with multiple receiving antenna used for simulation

As shown in the first system model, two transmitting antennas and one receiving antenna have been considered. Therefore, to transmit symbol 0, Tx1 (Transmitting antenna 1) is activated and to transmit symbol 1, Tx2 (Transmitting antenna 2) is activated. When there is activation of Tx1, the received signal is written as, $y_1 = \sqrt{E}h_1 + n$ and when there is activation of Tx2, the received signal is written as, $y_2 = \sqrt{E}h_2 + n$.

Table 2.1: SSK Mapping for single receiving antenna

symbol	Tx activated	Received Signal
0	1	$y_1 = \sqrt{E}h_1 + n$
1	2	$y_2 = \sqrt{E}h_2 + n$

Detection

For the detection of transmitted signal, ML detector has been used, which is as written below

$$u = arg \min_{j=1,2} \left(\left| y - \sqrt{E}h_j \right|^2 \right). \tag{2.2}$$

Assuming that, the data symbol to be transmitted is 0, resulting in the activation of Tx1. The received signal in this case can be written as

$$y_r = y_1 = \sqrt{E}h_1 + n. \tag{2.3}$$

If y_1 is the received signal, therefore, using ML detection method, the error can be defined as

$$P_e = P_r \left(\left| y_r - \sqrt{E}h_1 \right|^2 > \left| y_r - \sqrt{E}h_2 \right|^2 \right), \tag{2.4}$$

$$P_e = P_r \left(2\sqrt{E}\, \Re\left\{ (h_1 - h_2)\, n^* \right\} > \left| \sqrt{E}\, (h_1 - h_2) \right|^2 \right),$$

$$P_e = P_r \left(\left| \sqrt{E}\, (h_1 - h_2) \right|^2 < \hat{n} \right), \tag{2.5}$$

where, $\hat{n} = (2\sqrt{E}\, \Re\left\{ (h_1 - h_2)\, n^* \right\}$.

The variance of $\hat{n}$ can be computed as, $\sigma_n^2 = \mathbb{E}(\hat{n}^2)$, where, $\mathbb{E}$ is an Expectation operator. Therefore,

$$\sigma_n^2 = 4E\frac{N_0}{2}\left|h_1 - h_2\right|^2 = 2EN_0\left|h_1 - h_2\right|^2.$$

Hence, the Conditional Error Probability or Conditional Bit Error Rate (CBER) is defined as

$$P_r\left[n{>}a\right] = Q\left(\frac{a-\mu}{\sqrt{\sigma_N^2}}\right), \tag{2.6}$$

where, μ is the mean which is assumed as zero,

$$P_e = Q\left(\frac{E\left|h_1 - h_2\right|^2}{\sqrt{2EN_0\left|h_1 - h_2\right|^2}}\right),$$
$$P_e = Q\left(\sqrt{\frac{E^2\left|h_1 - h_2\right|^4}{2EN_0\left|h_1 - h_2\right|^2}}\right),$$

therefore, CBER can be computed as

$$P_e = Q\left(\sqrt{\frac{E\left|h_1 - h_2\right|^2}{2N_0}}\right) = Q\left(\sqrt{\frac{E\left|H\right|^2}{2N_0}}\right), \tag{2.7}$$

where, $H = h_1 - h_2$.

Now, CBER can be expressed in terms of γ as

$$P_e = Q\left(\sqrt{\gamma}\right), \tag{2.8}$$

where, $\gamma = \frac{E|h_1-h_2|^2}{2N_0} = \frac{E|H|^2}{2N_0}$, and $Q(x)$ is a gaussian Q function defined as

$$Q(x) = \frac{1}{\sqrt{2\pi}}\int_x^\infty \exp\left(\frac{-t^2}{2}\right)dt. \tag{2.9}$$

Probability Density Function (PDF)

The PDF of γ can be derived as follows

Firstly, the PDF of h is to be calculated, where, $h = x + jy$ (x is the real part and y is the imaginary part). Therefore, the joint PDF of x, y i.e $f_{XY}(x, y)$ can be written as

$$f_{XY}(x,y) = \frac{1}{\sqrt{2\pi\sigma_x^2}} \exp^{\frac{-(x-m)^2}{2\sigma_x^2}} \frac{1}{\sqrt{2\pi\sigma_y^2}} \exp^{\frac{-(y-m)^2}{2\sigma_y^2}}, \tag{2.10}$$

where, m is the mean, which has been considered zero for this analysis, $m = 0$ and σ^2 is the variance, which is considered equal for both x and y. Therefore, $\sigma_x^2 = \sigma_y^2 = \sigma^2$.
On substituting $m = o$, and $\sigma_x^2 = \sigma_y^2 = \sigma^2$ in (2.10)

$$f_{XY}(x,y) = \frac{1}{2\pi\sigma^2} \exp^{\frac{-(x+y)^2}{2\sigma^2}}.$$

Now, converting the above equation to polar co-ordinates.

Assuming, $a = |h| = \sqrt{x^2 + y^2}$ and $\theta = tan^{-1}\frac{y}{x}$, then,

$$f_{A\theta}(a,\theta) = \frac{1}{2\pi\sigma^2} \exp^{\frac{-a}{2\sigma^2}} J_{(x,y)},$$

where, $J_{(x,y)}$ is the Jacobian of x, y, which comes out to be $J_{(x,y)} = a$. Therefore, the above equation can be written as

$$f_{A\theta}(a,\theta) = \frac{a}{2\pi\sigma^2} \exp^{\frac{-a}{2\sigma^2}}. \tag{2.11}$$

From Eqn. (2.11), the individual PDF of $f_A(a)$ can be written as

$$f_A(a) = \int_0^{2\pi} \frac{a}{2\pi\sigma^2} \exp^{\frac{-a^2}{2\sigma^2}} d\theta,$$
$$f_A(a) = \frac{a}{\sigma^2} \exp^{\frac{-a^2}{2\sigma^2}}.$$

The above equation can be written in terms of x as follows

$$f_X(x) = \frac{x}{\sigma^2} \exp^{\frac{-x^2}{2\sigma^2}}. \tag{2.12}$$

As $\gamma = \frac{E|h|^2}{2N_0}$. Therefore, applying the Cumulative Distribution Function (CDF)

$$F_X(x) = Pr[X<x],$$
$$F_X(x) = Pr\left[\frac{E\,|h|^2}{2N_0}<x\right].$$

Let it be assumed that $\frac{E}{2N_0} = d$; therefore, $F_X(x)$ can be written as

$$F_X(x) = Pr\left[d\left|h\right|^2 < x\right],$$
$$F_X(x) = Pr\left[\left|h\right|^2 < \sqrt{\frac{x}{d}}\right]. \tag{2.13}$$

Equation 2.13, shows the expression of CDF, but we are interested in the PDF. Therefore, on differentiating (2.13)

$$F'_X(x) = \frac{1}{2d\sqrt{\frac{x}{d}}} f_X(x)dx. \tag{2.14}$$

On substituting, Eqn 2.12 in Eqn 2.14, the PDF can be written as

$$f_X(x) = F'_X(x) = \frac{1}{\frac{E\sigma^2}{N_0}} \exp^{\frac{\frac{x}{E\sigma^2}}{N_0}},$$

where $\frac{E\sigma^2}{N_0} = \bar{\gamma}$, therefore, PDF can further be computed as

$$f_\gamma\left(x\right) = \frac{1}{\bar{\gamma}} \exp\left(\frac{-x}{\bar{\gamma}}\right). \tag{2.15}$$

Average Bit Error Rate (ABER)

The ABER can be computed by averaging CBER given in (2.8) over the PDF of γ. Since H is circularly symmetric, Gaussian distributed and γ is Rayleigh distributed. Subsequently, its PDF can be written as

$$f_\gamma\left(\gamma\right) = \frac{1}{\bar{\gamma}} \exp\left(\frac{-\gamma}{\bar{\gamma}}\right), \tag{2.16}$$

where, $\bar{\gamma} = \mathbb{E}\left(\gamma\right) = \mathbb{E}\left(\frac{E|h_1 - h_2|^2}{2N_0}\right) = \mathbb{E}\left(\frac{E|H|^2}{2N_0}\right) = \frac{E\sigma^2}{N_0}$.

Average BER can be written as

$$ABER = \int_0^\infty P_e\left(\gamma\right) f_\gamma\left(\gamma\right) d\gamma, \tag{2.17}$$

where, $P_e\left(\gamma\right)$ is given in (2.8) and $f_\gamma\left(\gamma\right)$ is given in (2.16). Therefore, substituting (2.8) and (2.16) in (2.17), ABER can be written as

$$ABER = \int_0^\infty Q\left(\sqrt{\gamma}\right) \frac{1}{\bar{\gamma}} \exp\left(\frac{-\gamma}{\bar{\gamma}}\right) d\gamma. \tag{2.18}$$

On integrating (2.18), ABER can further be computed as

$$ABER = \frac{1}{2}\left(1 - \sqrt{\frac{\bar{\gamma}/2}{1+\bar{\gamma}/2}}\right),$$
$$ABER = \frac{1}{2}\left(1 - \sqrt{\frac{\bar{\gamma}}{2+\bar{\gamma}}}\right). \tag{2.19}$$

Simulation Results

In this section, MATLAB simulated result for ABER performance of SSK with perfect channel estimation and without any CCI for single receiving antenna are presented. In the simulation at least 10^6 channel realizations over the uncorrelated Rayleigh fading channel are considered. Furthermore, the simulation result is compared with the analytically derived result.

Fig. 2.7 shows the ABER versus SNR graph plotted for different values of SNR ranging from 0 dB to 30 dB. It can be clearly seen in the plot that simulation and analytical results are exactly overlapping each other, which indicates the accuracy of results. The graph depicts that as SNR increases, the ABER decreases, thus providing increase in the performance.

2.3.2 Asymptotic Analysis in Presence of Uncorrelated Rayleigh Fading Channels

By using the PDF given in (2.16), it is possible to numerically evaluate the system performance. However, these evaluations do not offer insight into how the system parameters are affected. Based on [56] and [42], the error probability in the fading channels depend on how the behavior of PDF is at the output SNR. It is seen that as SNR takes on larger values, the behavior of PDF becomes more irrelevant. This is due to the Q function approaching zero quickly, thus making the integrand almost null over the given integration range. But still, the behavior of PDF around zero is important since Q(0) = 1/2. The Taylor series can properly approximate this behavior and in general, the terms obtained from the Taylor series are easier to manipulate. Generally, for any large value of SNR, the PDF can be accurately approximated to the first term of Taylor series since the other terms are near zero. These arguments have been recognized by [56] and [42]. The approximate PDF of effective total SINR at the destination of the system is determined in this section by applying the Taylor series as in [57, 58].

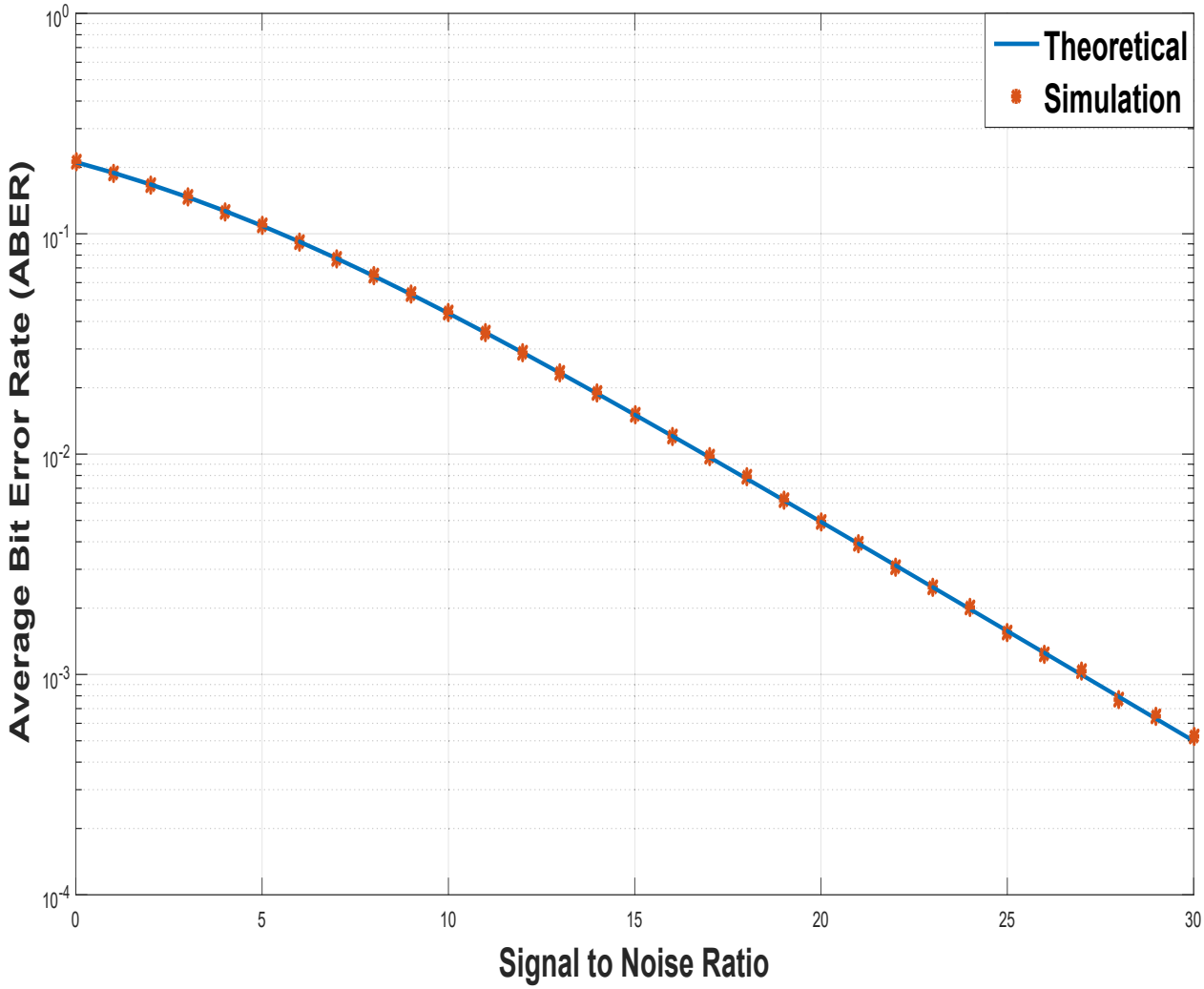

Figure 2.7: Analytical, Simulation results of ABER versus SNR for SSK system with no CCI over uncorrelated Rayleigh fading channels

From eqn. 2.15 and 2.16, the PDF can be written as

$$f_\gamma(\gamma) = \frac{1}{\bar{\gamma}} \exp\left(\frac{-\gamma}{\bar{\gamma}}\right),$$

where $\bar{\gamma} = \mathbb{E}(\gamma) = \mathbb{E}\left(\frac{E|h_1 - h_2|^2}{2N_0}\right) = \mathbb{E}\left(\frac{E|H|^2}{2N_0}\right) = \frac{E\sigma^2}{N_0}$.

Applying Taylor series expansion, the PDF can be written as

$$f_\gamma(\gamma) = \frac{1}{\bar{\gamma}} + HOT, \tag{2.20}$$

where, HOT refers to the Higher Order Terms.

Asymptotic ABER

Using the equation of ABER given in equation 2.17

$$ABER = \int_0^\infty P_e(\gamma) f_\gamma(\gamma) d\gamma, \tag{2.21}$$

where, $P_e(\gamma)$ is given in (2.8) and $f_\gamma(\gamma)$ is given in (2.20). Hence, neglecting the Higher Order Term of (2.20), asymptotic ABER can be written as:

$$AABER \simeq \int_0^\infty Q(\sqrt{\gamma}) \frac{1}{\bar{\gamma}} d\gamma, \tag{2.22}$$
$$AABER \simeq \frac{1}{\bar{\gamma}} \int_0^\infty Q(\sqrt{\gamma}) d\gamma.$$

On integrating the above equation Asymptotic ABER can be computed as

$$AABER \simeq \frac{1}{2\bar{\gamma}}. \tag{2.23}$$

Simulation Results

In this section, a comparison of exact theoretical and simulation ABER result with the asymptotic ABER result is provided. Asymptotic result is an approximate result which provides an idea of performance at high SNR.

It can be observed from Fig. 2.8 that the asymptotic result exactly overlaps the exact results in the region of high SNR. Therefore, asymptotic result is more tight at high SNR

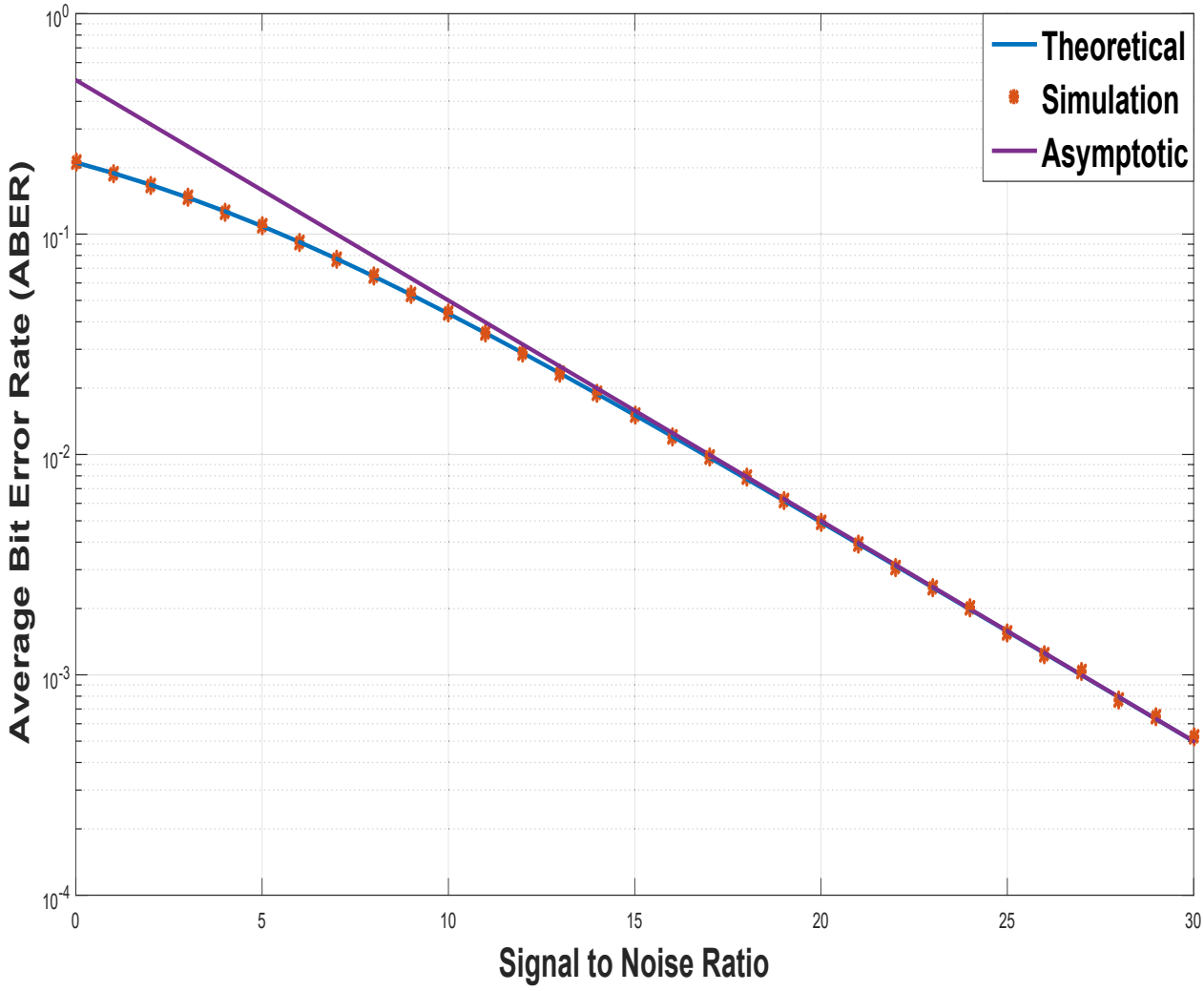

Figure 2.8: Comparison of Asymptotic and Exact results of ABER versus SNR for SSK system with no CCI over Uncorrelated Rayleigh fading channel

2.3.3 Exact Analysis in Presence of Correlated Rayleigh Fading Channels

In sections 2.3.1 and 2.3.2, it is assumed that fading channels are independent of each other. As the variance of $h_1 = 1$ and the variance of $h_2 = 1$, the resulting variance of $h_1 - h_2 = 2$. However, in this section, fading channels are assumed dependent on each other; in other words,

fading channels are correlated, with the resulting variance of $h_1 - h_2 \neq 2$.

The above-mentioned condition is commonly to be found in practical communication systems, especially in MIMO systems. Fading Correlation is caused due to the inadequate distance between the antennas, mainly in compact sized devices equipped with space-antenna diversity. It is important to analyze the performance of a system in the presence of Correlated Fading Channels because due to fading correlation, maximum diversity gain cannot be achieved.

In this section, the system as defined in section 2.3.1 has been analyzed assuming, the presence of Correlated Rayleigh fading channels, where ρ is the correlation coefficient.

Using the Eqn. 2.7 for CBER

$$P_e = Q\left(\sqrt{\frac{E\left|h_1 - h_2\right|^2}{2N_0}}\right) = Q\left(\sqrt{\frac{E\left|H\right|^2}{2N_0}}\right),$$

where, $H = h_1 - h_2$.
Similar to (2.8) CBER can be expressed in terms of γ_c

$$P_e = Q\left(\sqrt{\gamma_c}\right),$$

where, $\gamma_c = \frac{E|h_1 - h_2|^2}{2N_0}$. Using Eqn. 2.16 for the PDF

$$f_{\gamma_c}\left(\gamma_c\right) = \frac{1}{\bar{\gamma_c}} \exp\left(\frac{-\gamma_c}{\bar{\gamma_c}}\right),$$

where, $\bar{\gamma_c} = \mathbb{E}\left(\gamma_c\right) = \mathbb{E}\left(\frac{E|h_1 - h_2|^2}{2N_0}\right) = \mathbb{E}\left(\frac{E|H|^2}{2N_0}\right) = \frac{E\sigma^2}{N_0}\left(1 - \rho\right)$,
where, ρ is the coefficient of Correlation between fading channels and σ^2 is the variance of each fading channel; therefore, $\sigma^2 = 1$.

Average Bit Error Rate (ABER)

ABER can be written as given (2.17)

$$ABER = \int_0^\infty P_e(\gamma_c) f_{\gamma_c}(\gamma_c) d\gamma_c$$
$$ABER = \int_0^\infty Q(\sqrt{\gamma_c}) \frac{1}{\bar{\gamma}_c} \exp\left(\frac{-\gamma_c}{\bar{\gamma}_c}\right) d\gamma_c. \quad (2.24)$$

ABER can be computed as

$$ABER = \frac{1}{2}\left(1 - \sqrt{\frac{\bar{\gamma}_c/2}{1+\bar{\gamma}_c/2}}\right) = \frac{1}{2}\left(1 - \sqrt{\frac{\bar{\gamma}_c}{2+\bar{\gamma}_c}}\right), \quad (2.25)$$

where, $\bar{\gamma}_c = \frac{E}{N_0}(1-\rho)$.

Simulation Results

In this section, MATLAB simulated results for exact ABER performance of SSK in the presence of Correlated Rayleigh Fading Channels are provided. The results for different values of correlation coefficient (ρ) are provided in order to study the effect of fading correlation on the performance of the system.

Fig. 2.9 demonstrates that the fading correlation and ABER are directly proportional. As the value of correlation coefficient increases, the performance decreases. It can be noted from the figure that, for $\rho = 0$ i.e when there is no correlation between fading channels or they are completely independent, the ABER of 10^{-2} is obtained at SNR = 17dB, and for $\rho = 0.3$, the ABER of 10^{-2} is achieved at SNR = 18dB, which shows the loss of 1dB. However, on further increasing the value of ρ to 0.6 and 0.9, the ABER of 10^{-2} is achieved at SNR of 21dB and 27dB, thus showing the loss by 4dB and 10dB respectively.

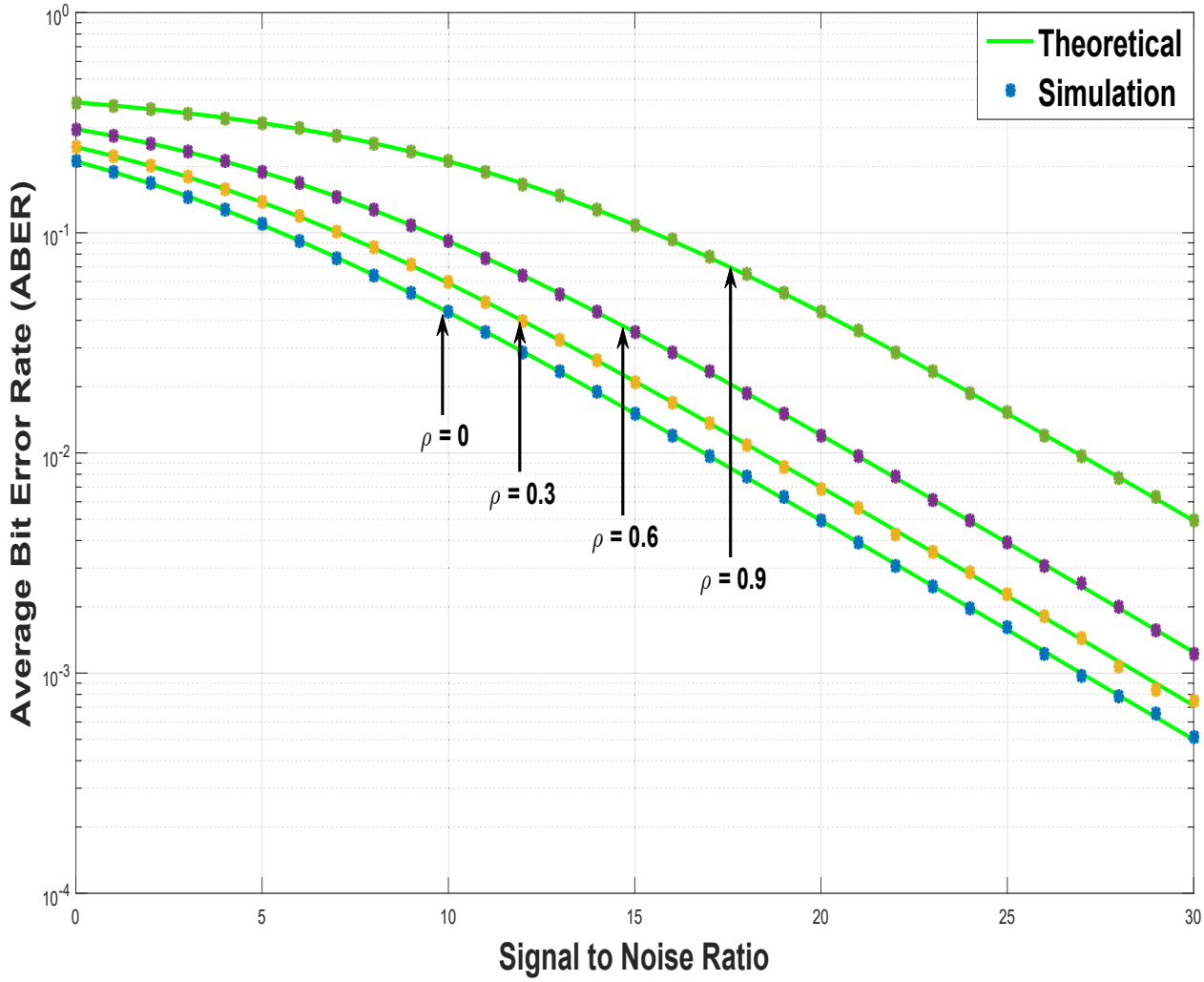

Figure 2.9: Analytical, Simulation results of ABER versus SNR for SSK system with no interference over Correlated Rayleigh fading channels

2.4 Performance Analysis for Multiple Receiving Antenna with Perfect CSI and no Co-channel Interferer

2.4.1 Exact Analysis in Presence of Uncorrelated Rayleigh Fading Channels

Transmission and Reception

In this section, performance analysis for a system with multiple receiving antennas has been studied, using MRC based ML detector.

The received signal at receiving end can be written as

$$y_r = \sqrt{E}h_{r,t} + n_r, \qquad t = 1, 2, \tag{2.26}$$

where, r is the receiving antenna, t is the transmitting antenna, $\sqrt{E}$ is the energy of desired signal, $h_{r,t}$ is the complex Gaussian Rayleigh fading channel of activated transmitting antenna and r^{th} receiving antenna with mean zero and variance 1, $h_{r,t} \sim \mathcal{CN}\ (0, 1)$ and n is complex Gaussian white noise with mean 0 and variance N_0, $n \sim \mathcal{CN}\ (0, N_0)$.

As shown in the second model, two transmitting antennas and N_r receiving antennas has been considered. Therefore, to transmit symbol 0, Tx1 (Transmitting antenna 1) is activated and to transmit symbol 1, Tx2 (Transmitting antenna 2) is activated. On the activation of Tx1, $y_{r,1} = \sqrt{E}h_{r,1} + n_r$, is received at the receiving antennas and on activation of Tx2, $y_{r,2} = \sqrt{E}h_{r,2} + n_r$, is received at the receiving antennas.

Table 2.2: SSK Mapping for multiple receiving antennas

symbol	Tx activated	Received Signal at r^{th} Receive Antenna
0	1	$y_{r,1} = \sqrt{E}h_{r,1} + n_r$
1	2	$y_{r,2} = \sqrt{E}h_{r,2} + n_r$

Detection

ML detector, used for the detection of transmitted signal is defined as

$$u = arg \min_{t=1,2} \left(\sum_{r=1}^{N_r} \left| y_r - \sqrt{E} h_{r,t} \right|^2 \right). \tag{2.27}$$

Assuming that 0 is the symbol to be transmitted, resulting in the activation of Tx1. In this case, received signal at the r^{th} antenna can be written as

$$y_r = \sqrt{E} h_{r,1} + n_r. \tag{2.28}$$

As, y_1 is the received signal, therefore, using ML detection method, the error can be defined as

$$P_e = P_r \left(\sum_{r=0}^{N_r} \left| y_1 - \sqrt{E} h_{r,1} \right|^2 > \sum_{r=0}^{N_r} \left| y_1 - \sqrt{E} h_{r,2} \right|^2 \right), \tag{2.29}$$

$$P_e = P_r \left(2\sqrt{E}\, \Re \left\{ \sum_{r=0}^{N_r} \left(h_{r,1} - h_{r,2} \right) n_r^* \right\} > \sum_{r=0}^{N_r} \left| \sqrt{E} \left(h_{r,1} - h_{r,2} \right) \right|^2 \right),$$

$$P_e = P_r \left(\sum_{r=0}^{N_r} \left| \sqrt{E} \left(h_{r,1} - h_{r,2} \right) \right|^2 < \hat{n} \right), \tag{2.30}$$

where $\hat{n} = 2\sqrt{E}\, \Re \left\{ \sum_{r=0}^{N_r} \left(h_{r,1} - h_{r,2} \right) n_r^* \right\}$.

The variance of $\hat{n}$ can be computed as, $\sigma_n^2 = \mathbb{E}\left(\hat{n}^2\right)$, where $\mathbb{E}$ is an Expectation operator. Therefore,

$$\sigma_n^2 = 4E \frac{N_0}{2} \sum_{r=0}^{N_r} \left| h_{r,1} - h_{r,2} \right|^2,$$

$$\sigma_n^2 = 2EN_0 \sum_{r=0}^{N_r} \left| h_{r,1} - h_{r,2} \right|^2.$$

Hence, the Conditional Error Probability is defined as

$$P_r \left[n > a \right] = Q \left(\frac{a - \mu}{\sqrt{\sigma_N^2}} \right), \tag{2.31}$$

where, μ is the mean which is assumed as zero.

$$P_e = Q\left(\frac{\sum_{r=0}^{N_r} E\left|h_{r,1}-h_{r,2}\right|^2}{\sqrt{\sum_{r=0}^{N_r} 2EN_0\left|h_{r,1}-h_{r,2}\right|^2}}\right),$$

$$P_e = Q\left(\sqrt{\frac{\sum_{r=0}^{N_r} E^2\left|h_{r,1}-h_{r,2}\right|^4}{2EN_0\sum_{r=0}^{N_r}\left|h_{r,1}-h_{r,2}\right|^2}}\right). \tag{2.32}$$

Therefore, CBER be written as

$$P_e = Q\left(\sqrt{\frac{\sum_{r=0}^{N_r} E\left|h_{r,1}-h_{r,2}\right|^2}{2N_0}}\right), \tag{2.33}$$

Now, CBER can be expressed in terms of γ_r as

$$P_e = Q\left(\sqrt{\gamma_r}\right), \tag{2.34}$$

where, $\gamma_r = \frac{\sum_{r=0}^{N_r} E|h_{r,1}-h_{r,2}|^2}{2N_0}$, and $Q(x)$ is a gaussian Q function defined in (2.9) as

$$Q(x) = \frac{1}{\sqrt{2\pi}}\int_x^\infty \exp\left(\frac{-t^2}{2}\right)dt. \tag{2.35}$$

Probability Density Function (PDF)

The PDF of γ_r can be written by using [43, 14-4-13] as

$$f_{\gamma r}(\gamma_r) = \frac{1}{(N_r-1)!}\left(\frac{1}{\bar{\gamma_r}}\right)^{N_r}\gamma_r^{N_r-1}\exp\left(\frac{-\gamma_r}{\bar{\gamma_r}}\right), \tag{2.36}$$

where $\bar{\gamma_r} = \mathbb{E}(\gamma_r) = \mathbb{E}\left(\frac{\sum_{r=0}^{N_r} E|h_{r,1}-h_{r,2}|^2}{2N_0}\right)$.

Average Bit Error Rate (ABER)

The ABER can be computed by averaging CBER in (2.34) over the PDF of γ_r given in (2.36).

Hence, the ABER can be computed as in (2.17). Therefore, substituting (2.34) and (2.36) in (2.17) ABER can be written as

$$ABER = \int_0^\infty Q\left(\sqrt{\gamma_r}\right)\frac{1}{(N_r-1)!}\left(\frac{1}{\bar{\gamma_r}}\right)^{N_r}\gamma_r^{N_r-1}\exp\left(\frac{-\gamma_r}{\bar{\gamma_r}}\right)d\gamma_r, \tag{2.37}$$

$$ABER = \gamma_a^{N_r}\sum_{k=0}^{N_r-1}\binom{N_r-1+k}{k}\left[1-\gamma_a\right]^k, \tag{2.38}$$

where $\gamma_a = \frac{1}{2}\left(1-\sqrt{\frac{\bar{\gamma_b}/2}{1+\bar{\gamma_b}/2}}\right) = \frac{1}{2}\left(1-\sqrt{\frac{\bar{\gamma_b}}{2+\bar{\gamma_b}}}\right)$, where $\bar{\gamma_b} = \frac{\bar{\gamma_r}}{N_r}$.

Simulation Results

In this section, the MATLAB simulated result for ABER performance of SSK without any CCI for multiple receiving antennas has been provided. At least 10^6 channel realizations over the Rayleigh fading channel are considered for this simulation. Furthermore, simulation and analytically derived results are compared.

Fig. 2.10 shows the ABER versus SNR plot for different values of SNR ranging from 0 dB to 30 dB. This figure is plotted for the variable number of receiving antennas, varying from $N_r = 1$ to $N_r = 5$, in order to study the effects of increase/decrease in the number of receiving antennas or the receive diversity. It can be seen that the simulated and analytical results are similar, which is the evidence for the accuracy of the theoretical result. The graph depicts that as SNR increases, the average bit error rate decreases, thus giving an increase in performance. Also, on an increase in the number of receiving antennas, a decrease in ABER is observed, resulting in better performance. It can be said that with more receiving antennas, the less signal power is needed for high performance. It is observed from the figure that, to obtain the ABER of 10^{-3}, different SNR is needed, depending on the number of receiving antennas in the system.

In the case of 1 receiving antenna; i.e., if $N_r = 1$, there is a need for around 27dB of SNR to obtain ABER of 10^{-3}dB. Whereas, in the case of $N_r = 2$ there is a need of around 14dB of SNR, which shows a gain of 13dB. Similarly, if there are five receiving antennas, i.e., $N_r = 5$, then 5.5dB of SNR is needed to obtain the ABER of 10^{-3}, which provides a gain of 27.5dB when compared to the case of $N_r = 1$.

It is clearly visible from the figure 2.10 that, there is the biggest gap in the curve for $N_r = 1$ and $N_r = 2$, therefore, showing the significant increase in the performance. However, as the value of N_r is increasing, the gap of the curve when compared with the curve of the adjacent lower value of N_r goes on decreasing which shows that as we increase the number of antennas so does the performance increases but the increase in performance is getting limited or the gain in

SNR is decreasing.

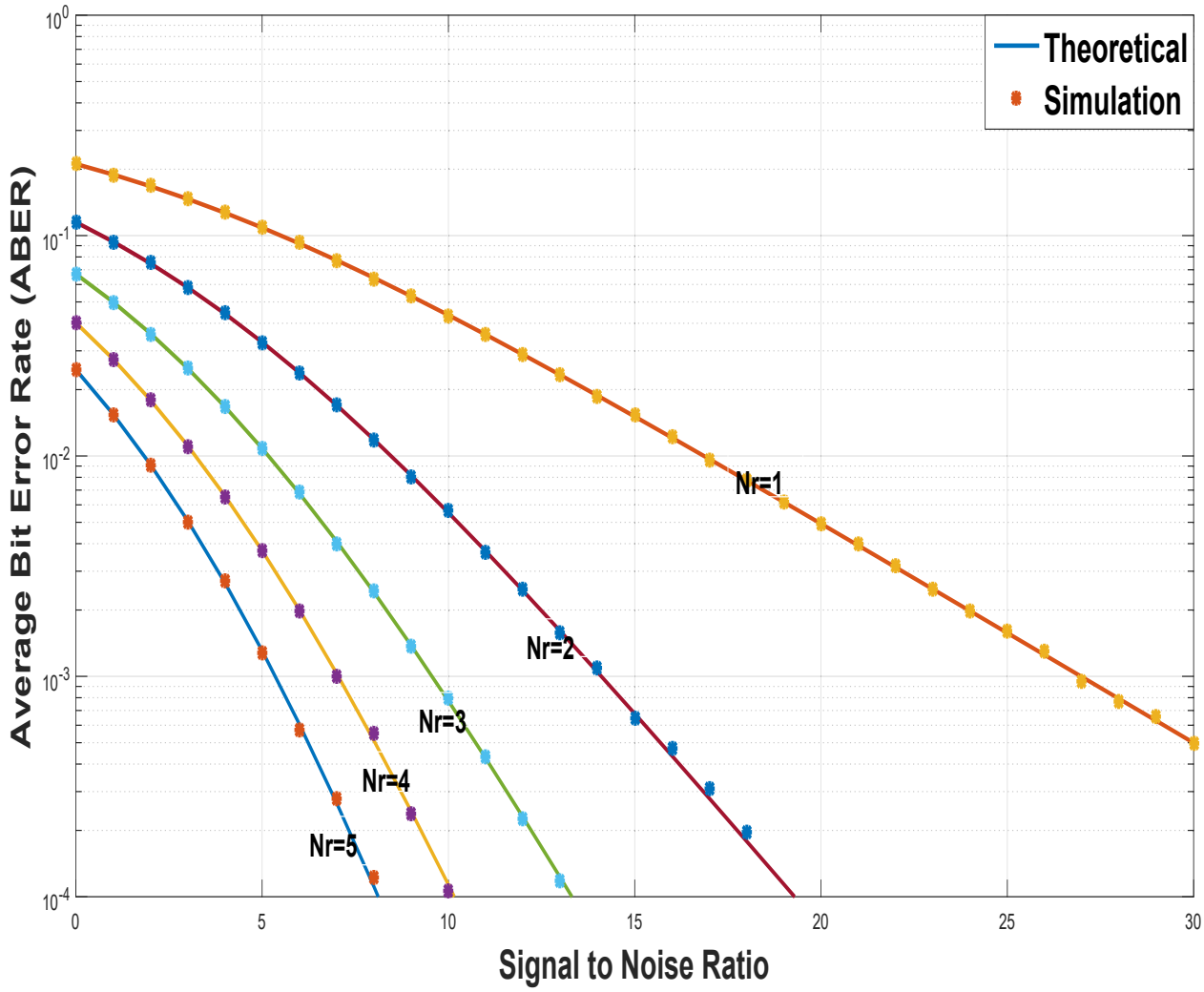

Figure 2.10: Analytical, Simulation results of ABER versus SNR of SSK system with no interference over Uncorrelated Rayleigh fading channels

2.4.2 Asymptotic Analysis in Presence of Uncorrelated Rayleigh Fading Channels

Using the Conditional Error Probability given in (2.33)

$$P_e = Q\left(\sqrt{\frac{\sum_{r=0}^{N_r} E\left|h_{r,1} - h_{r,2}\right|^2}{2N_0}}\right),$$

Similar to (2.34), above equation can further be expressed in terms of γ_r as

$$P_e = Q\left(\sqrt{\gamma_r}\right), \tag{2.39}$$

where $\gamma_r = \frac{\sum_{r=0}^{N_r} E|h_{r,1}-h_{r,2}|^2}{2N_0}$.

Using the PDF given in (2.36)

$$f_{\gamma_r}(\gamma_r) = \frac{1}{(N_r-1)!}\left(\frac{1}{\bar{\gamma_r}}\right)^{N_r} \gamma_r^{N_r-1} \exp\left(\frac{-\gamma_r}{\bar{\gamma_r}}\right). \tag{2.40}$$

On applying Taylor series expansion and similar to [39, 12], the above equation can be written as

$$f_{\gamma_r}(\gamma_r) = \frac{1}{(N_r-1)!}\left(\frac{1}{\bar{\gamma_r}}\right)^{N_r} \gamma_r^{N_r-1} + H.O.T, \tag{2.41}$$

where H.O.T stands for Higher Order Terms and $\bar{\gamma_r} = \mathbb{E}(\gamma_r) = \mathbb{E}\left(\frac{\sum_{r=0}^{N_r} E|h_{r,1}-h_{r,2}|^2}{2N_0}\right)$.

Asymptotic ABER

Now, Substituting (2.39) and the first term of (2.41) in (2.17), asymptotic ABER can be written as

$$AABER = \int_0^\infty Q\left(\sqrt{\gamma_r}\right) \frac{1}{(N_r-1)!}\left(\frac{1}{\bar{\gamma_r}}\right)^{N_r} \gamma_r^{N_r-1} d\gamma_r.$$

On solving the integral, above equation can be computed as

$$AABER = \frac{1}{N_r!}\left(\frac{1}{\bar{\gamma_r}}\right)^{N_r} \frac{2^{(N_r-1)}\Gamma(N_r+0.5)}{\sqrt{\pi}} = C\left(\frac{1}{\bar{\gamma_r}}\right)^{N_r}, \tag{2.42}$$

where $C = \frac{1}{N_r!}\frac{2^{(N_r\ \ 1)}\Gamma(N_r+0.5)}{\sqrt{\pi}}$, is a constant. Beign a constant relying on the number of receiving antennas N_r, 2.42 clearly indicates that the diversity order equal to the number of receiving antennas N_r can be obtained.

Simulation Results

In this section, a plot showing the comparison of exact performance analysis with the asymptotic analysis is provided. Asymptotic results are approximate results used to study the performance

of the system at high SNR. In Fig. 2.11, results are presented considering variable number of number of receiving antennas, varying from $N_r = 1 - 5$.

It can be seen in the figure that, for $N_r = 1$ the asymptotic result starts overlapping the exact result from SNR = 17dB, whereas, for $N_r = 2$ the results start overlapping from SNR= 20dB which goes on increasing as there is an increase in the number of receiving antennas. Therefore, it can be said that asymptotic result loses its tightness with increase in receive diversity.

2.4.3 Exact Analysis in Presence of Correlated Rayleigh Fading Channels

Using (2.33), the CBER can be written as

$$P_e = Q\left(\sqrt{\frac{\sum_{r=0}^{N_r} E\left|h_{r,1} - h_{r,2}\right|^2}{2N_0}}\right), \tag{2.43}$$

Now, similar to (2.34), CBER can be expressed in terms of γ_{rc} as

$$P_e = Q\left(\sqrt{\gamma_{rc}}\right), \tag{2.44}$$

where $\gamma_{rc} = \frac{\sum_{r=0}^{N_r} E|h_{r,1}-h_{r,2}|^2}{2N_0}$.

Using (2.36), PDF can be written as

$$f_{\gamma_{rc}}\left(\gamma_{rc}\right) = \frac{1}{(N_r-1)!}\left(\frac{1}{\bar{\gamma_{rc}}}\right)^{N_r} \gamma_r^{N_r-1} \exp\left(\frac{-\gamma_{rc}}{\bar{\gamma_{rc}}}\right), \tag{2.45}$$

where, $\bar{\gamma_{rc}} = \mathbb{E}\left(\gamma_{rc}\right) = \mathbb{E}\left(\frac{\sum_{r=0}^{N_r} E|h_{r,1}-h_{r,2}|^2}{2N_0}\right) = \frac{N_r E\sigma_r^2}{N_0}\left(1-\rho_r\right)$,
where, N_r is number of receiving antennas, σ_r^2 is the variance of each fading channel = 1, and ρ_r is the correlation coefficient between fading channels.

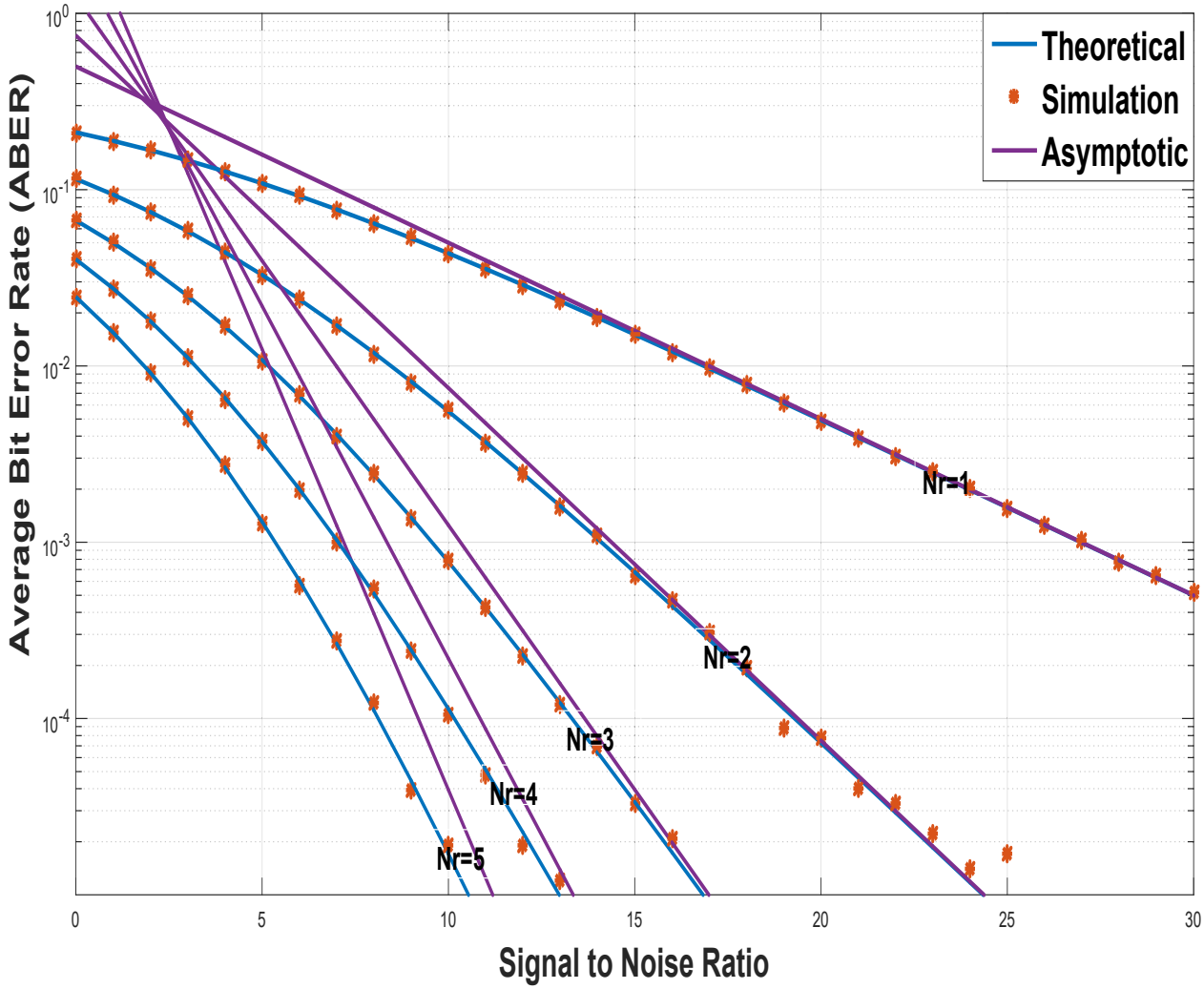

Figure 2.11: Comparison of Asymptotic and Exact results of ABER v/s SNR for SSK system with no interference over Uncorrelated Rayleigh channels

Average Bit Error Rate (ABER)

Using Eqn. 2.17 and similar to 2.37, the ABER can be computed by substituting 2.44 and 2.45 in 2.17

$$ABER = \int_0^\infty Q\left(\sqrt{\gamma_{rc}}\right) \frac{1}{(N_r-1)!} \left(\frac{1}{\bar{\gamma_{rc}}}\right)^{N_r} \gamma_{rc}^{N_r-1} \exp\left(\frac{-\gamma_{rc}}{\bar{\gamma_{rc}}}\right) d\gamma_{rc},$$

$$ABER = \gamma_{ac}^{N_r} \sum_{k=0}^{N_r-1} \binom{N_r-1+k}{k} \left[1-\gamma_{ac}\right]^k, \tag{2.46}$$

where, $\gamma_{ac} = \frac{1}{2}\left(1 - \sqrt{\frac{\bar{\gamma_{bc}}/2}{1+\bar{\gamma_{bc}}/2}}\right) = \frac{1}{2}\left(1 - \sqrt{\frac{\bar{\gamma_{bc}}}{2+\bar{\gamma_{bc}}}}\right)$,
where, $\bar{\gamma_{bc}} = \frac{\bar{\gamma_{rc}}}{N_r}$, and $\bar{\gamma_{rc}} = \frac{N_r E}{N_0}\left(1-\rho_r\right)$.

Simulation Results

In this section, MATLAB plotted simulation and analytical results for ABER in the presence of correlated Rayleigh fading channels are presented. The results are provided by varying the values of correlation coefficient for a different number of receiving antennas.

It can be seen in Fig. 2.12 that as the value of correlation coefficient increases, the performance of the system decreases whereas the performance of the system is enhanced by increasing number of receiving antennas. The results are provided assuming 1, 3, and 5 are the number of receiving antennas with the correlation coefficient (ρ) = 0, 0.5 and 0.9 for each number of receiving antennas.

As per the results illustrated in Fig. 2.12, it can be said that the system with $N_r = 1$ and $\rho = 0.9$ is the system with the lowest performance among all the systems shown. However, the system with $N_r = 5$ and $\rho = 0$ is the system with highest performance or with most efficiency among all the systems shown.

It can be seen that for $N_r = 5$, on increasing the value of ρ the gap between curves is greater as compared to the gap between the curves for $N_r = 3$. The least gap between the curves occurs for $N_r = 1$. Therefore, it can be said that with an increase in the number of receiving antennas

the effect of correlation also increases. The figure also depicts that an effect of correlation also increases with an increase in SNR, as the gap between the curves of different values of ρ keeps on increasing with an increase in SNR for each value of N_r.

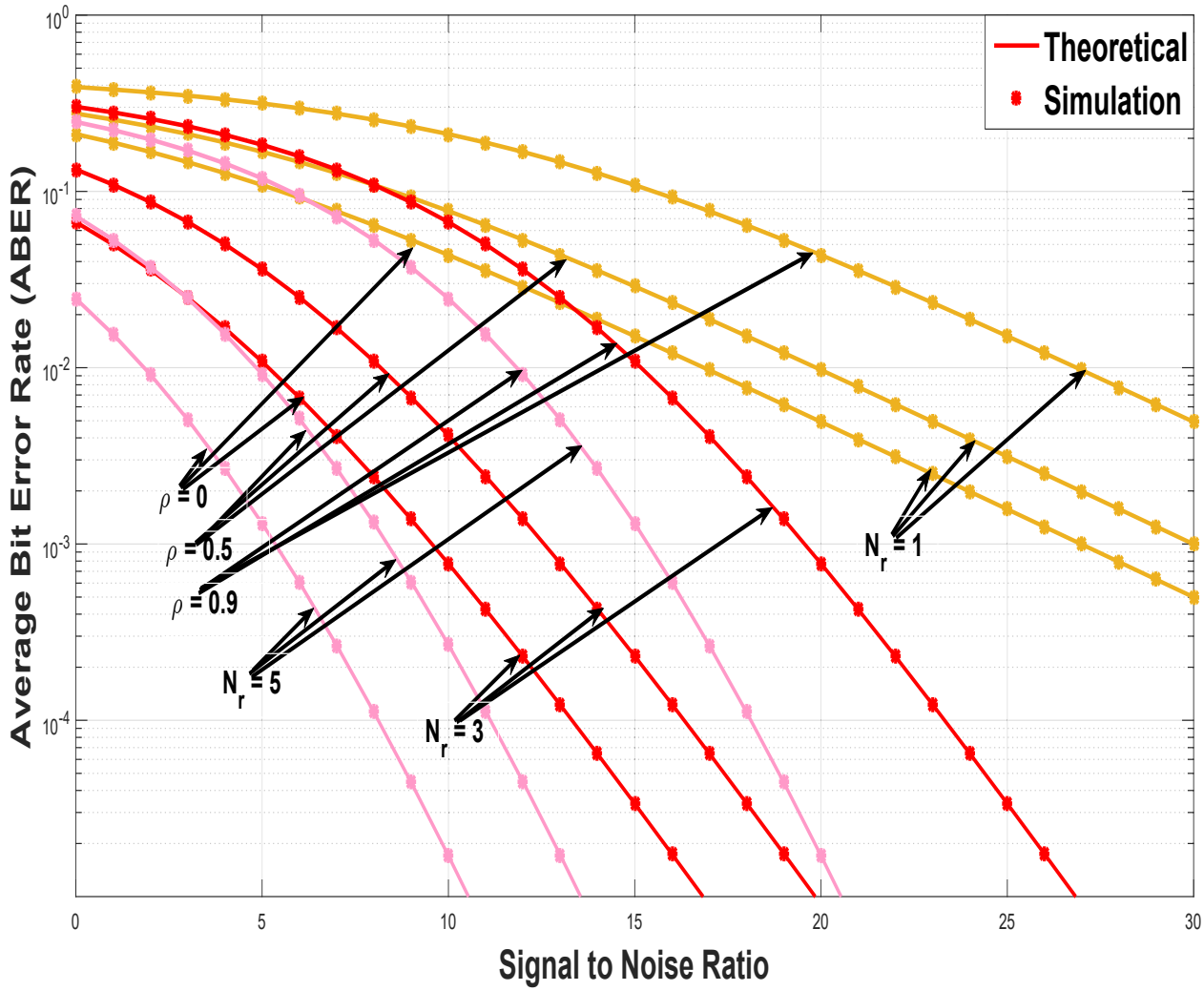

Figure 2.12: Analytical, Simulation results of ABER versus SNR for SSK system with no CCI over correlated Rayleigh fading channels

Chapter 3

Space Shift Keying Modulation in Presence of Multiple Co-Channel Interferers

In this chapter, the performance of SSK Modulation in presence of multiple co-channel interferers has been studied.

This chapter is divided into two sections. In the first section, performance is studied assuming single receiving antenna and in the second section, multiple receiving antennas are assumed. In both the sections, exact expressions for ABER over correlated and uncorrelated Rayleigh fading channel using the ML detection method are derived. Also, the expressions for asymptotic ABER are provided. Throughout the analysis, equal power multiple co-channel interferers are assumed.

3.1 System Model

3.1.1 Single Receiving Antenna

Shown in Fig. 3.1 an 3.2 is the first system with two transmitting antennas and a single receiving antenna. Similarly, as mentioned before in chapter 2 section 2.1.1, that in SSK system only one transmitting antenna is in a state of action at a time. Fig. 3.1 refers to the time instance, when 0 is the data to be transmitted; therefore, transmitting antenna Tx1 is in active mode and

Tx2 is in sleep mode. Similarly, Fig. 3.2 shows the time instance, when 1 is the data to be transmitted, therefore, transmitting antenna Tx2 is in active mode and Tx1 is in sleep mode. In this system model, L equal power co-channel interferers are assumed to affect the received signal.

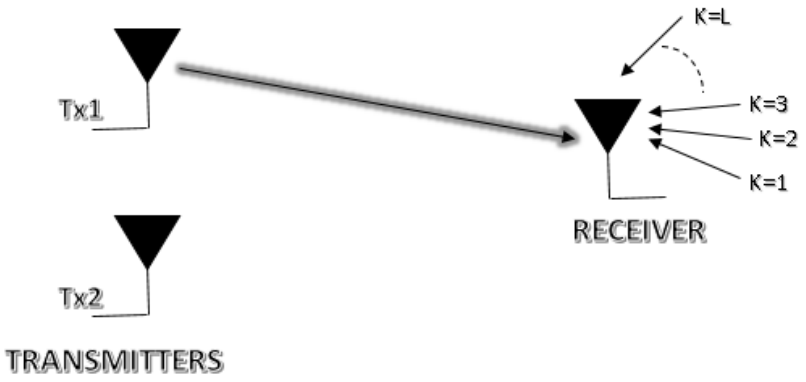

Figure 3.1: When transmitting data= 0, single receiving antenna in presence of CCI

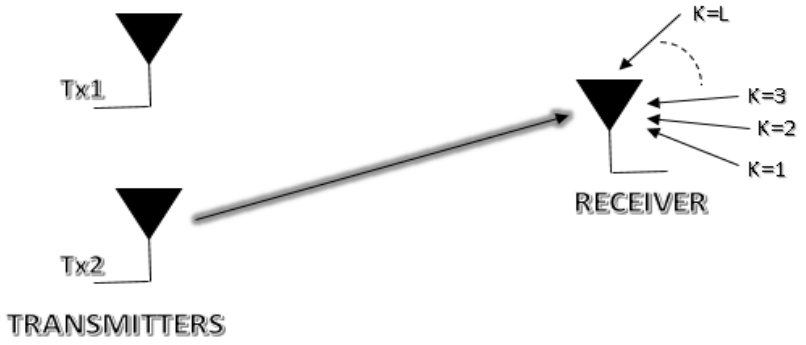

Figure 3.2: When transmitting data= 1, single receiving antenna in presence of CCI

3.1.2 Multiple Receiving Antennas

The second system is shown in Fig. 3.3 and 3.4. In this system, two transmitting antennas and N_r(multiple) receiving antennas are considered. In this system, MRC is used as diversity combining scheme. These figures 3.3 and 3.4 gives an idea for the working of antennas. The working of antennas is very similar to what was described in section 2.1.2. Fig. 3.3 shows the

time, when 0 is the data to be transmitted, which activates transmitting antenna Tx1 to transmit data over all the receiving antennas, whereas, Tx2 is in sleep mode. Therefore, there is no data transmission from Tx2. Similarly, Fig. 3.4 shows the time when transmitting antenna Tx2 is in active mode and Tx1 is in sleep mode, and this happens when 1 is the data to be transmitted. In both of these conditions each of the received signal is exposed to L equal power co-channel interferers.

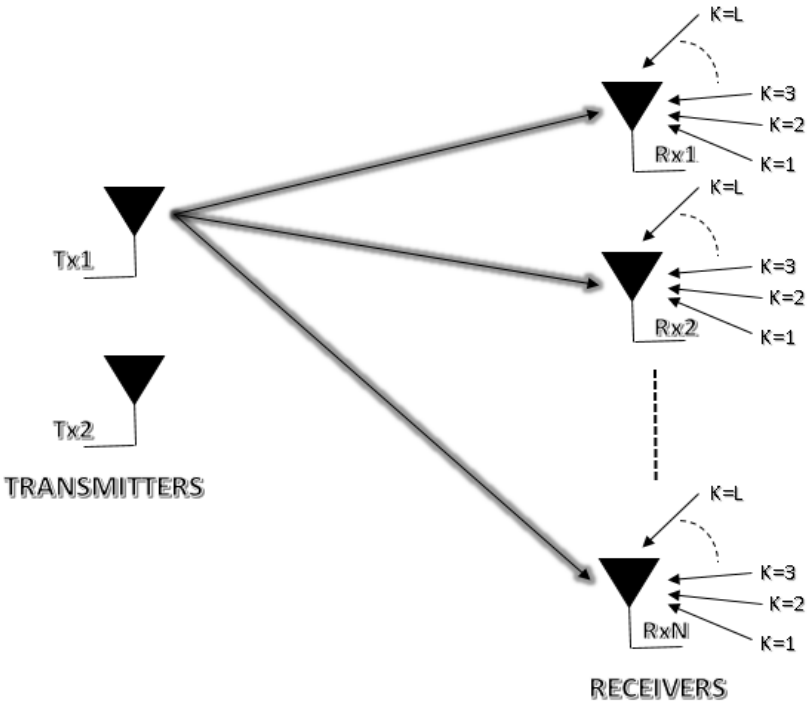

Figure 3.3: When transmitting data= 0, Multiple receiving antennas in presence of CCI

3.2 System Model for Simulation

3.2.1 Single Receiving Antenna

Figure 3.5 shows the system model with single receiving antenna developed for the simulations in MATLAB.

3.2.2 Multiple Receiving Antennas

Figure 3.6 shows the system model with multiple receiving antennas developed for the simulations in MATLAB.

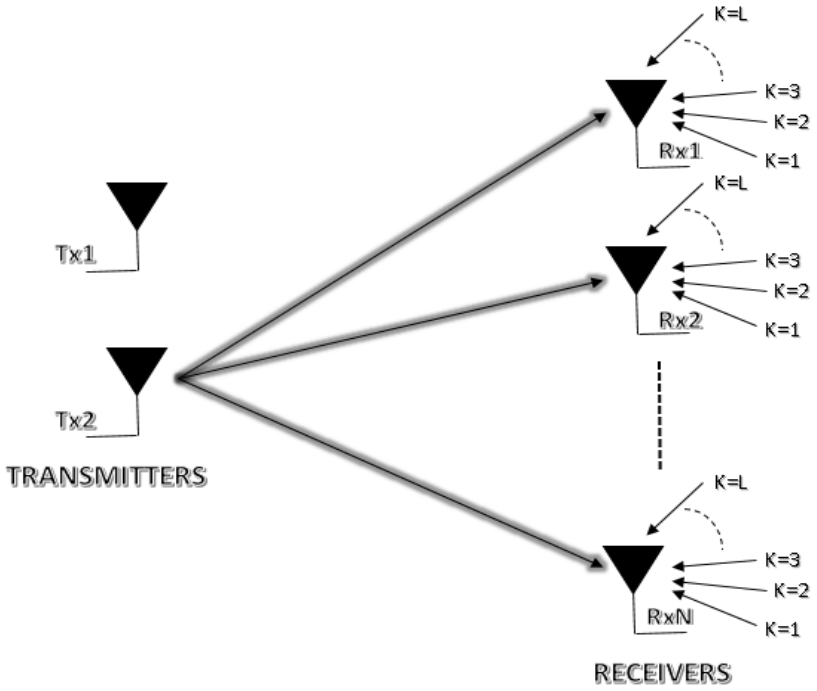

Figure 3.4: When transmitting data= 1, Multiple receiving antennas in presence of CCI

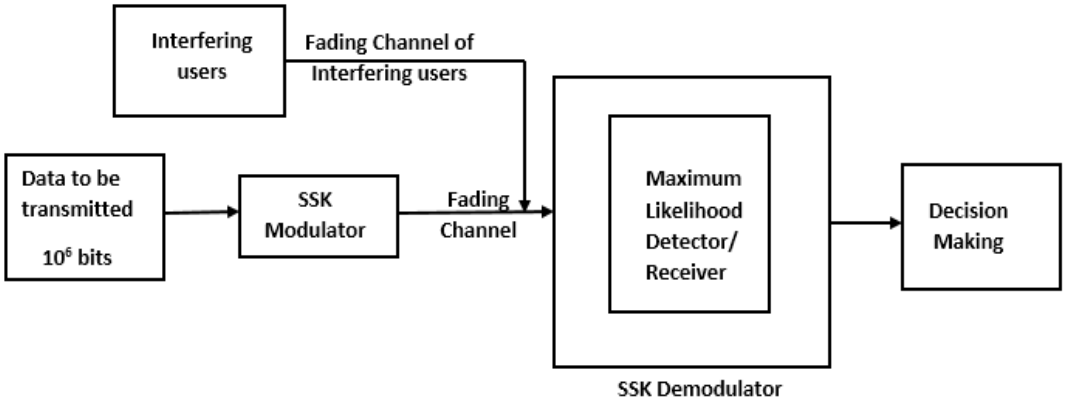

Figure 3.5: Block diagram of system with single receiving antenna used for simulation

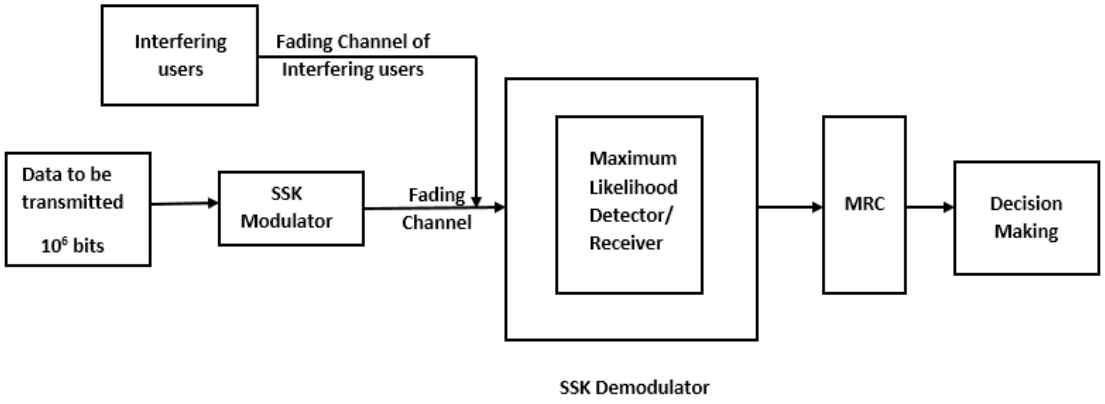

Figure 3.6: Block diagram of system with multiple receiving antenna used for simulation

3.3 Performance Analysis for Single Receiving Antenna with Perfect CSI and Multiple Co-channel interferers

3.3.1 Exact Analysis in Presence of Uncorrelated Rayleigh Fading Channels

Transmission and Reception

The received signal at the receiving antenna is

$$y = \sqrt{E_s}h_j + \sum_{k=1}^{L} \sqrt{E_{ik}}g_k + w, \qquad j = 1, 2, \tag{3.1}$$

where, $\sqrt{E_s}$ is the energy of desired signal, $\sqrt{E_{ik}}$ is the energy of k^{th} interfering user, w is the complex Gaussian white noise, with mean zero and variance N_0, $N_0 \sim \mathcal{CN}(0, N_0)$ h_j and g_k are the complex Gaussian Rayleigh fading channel of activated user antenna and the k^{th} interfering user with mean zero and variance 1, $h_j \sim \mathcal{CN}(0, 1)$, $g_k \sim \mathcal{CN}(0, 1)$. Both h_j and g_k are considered mutually independent of each other. Perfect channel estimation is assumed at the receiving end.

In first model, two transmitting antenna and one receiving antenna is considered. Therefore, to transmit symbol 0, Tx1 is activated and to transmit symbol 1, Tx2 is activated and if data is transmitted by Tx1 then, $y_1 = \sqrt{E_s}h_1 + \sum_{k=1}^{L} \sqrt{E_{ik}}g_k + w$ is the received signal and if data is transmitted by Tx2 then, $y_2 = \sqrt{E_s}h_2 + \sum_{k=1}^{L} \sqrt{E_{ik}}g_k + w$ is the received signal.

Table 3.1: SSK Mapping for single receiving antenna with CCI

symbol	Tx activated	Received Signal
0	1	$y_1 = \sqrt{E_s}h_1 + \sum_{k=1}^{L}\sqrt{E_{ik}}g_k + w$
1	2	$y_2 = \sqrt{E_s}h_2 + \sum_{k=1}^{L}\sqrt{E_{ik}}g_k + w$

Detection

ML detector written below, has been used to detect the transmitted signal

$$u = arg\min_{j=1,2}\left(\left|y - \sqrt{E_s}h_j\right|\right). \tag{3.2}$$

Assuming that the symbol to be transmitted is 0, resulting in the activation of Tx1, the received signal in this case can be written as

$$y_r = y_1 = \sqrt{E_s}h_1 + \sum_{k=1}^{L}\sqrt{E_{ik}}g_k + w. \tag{3.3}$$

In case, y_1 is the received signal, therefore, using ML detection method, the error can be defined as

$$P_e = P_r\left(\left|y_r - \sqrt{E_s}h_1\right|^2 > \left|y_r - \sqrt{E_s}h_2\right|^2\right), \tag{3.4}$$

$$P_e = P_r\left(\left(2\sqrt{E_s}\Re\left(h_1 - h_2\right)w^* + \left(h_1 - h_2\right)\sum_{k=1}^{L}\sqrt{E_{ik}}g_k^*\right) > \left|\sqrt{E_s}\left(h_1 - h_2\right)\right|^2\right),$$

$$P_e = P_r\left(\left|\sqrt{E_s}\left(h_1 - h_2\right)\right|^2 < \hat{w}\right), \tag{3.5}$$

where, $\hat{w} = \left(2\sqrt{E_s}\Re\left(h_1 - h_2\right)w^* + \left(h_1 - h_2\right)\sum_{k=1}^{L}\sqrt{E_{ik}}g_k^*\right)$.

The variance of $\hat{w}$ can be computed as : $\sigma_w^2 = \mathbb{E}\left(\hat{w}^2\right)$, where $\mathbb{E}$ is an Expectation operator. Therefore,

$$\sigma_w^2 = 4E_s\left|h_1 - h_2\right|^2\left[\frac{N_0}{2} + \sum_{k=1}^{L}\frac{\sqrt{E_{ik}}\left|g_k\right|^2}{2}\right],$$

$$\sigma_w^2 = 2E_s\left|h_1 - h_2\right|^2\left[N_0 + \sum_{k=1}^{L}\sqrt{E_{ik}}\left|g_k\right|^2\right].$$

Hence, using (2.6) CBER can be written as

$$P_e = Q\left(\frac{\left|\sqrt{E_s}\left(h_1 - h_2\right)\right|^2}{\sqrt{2E_s\left|h_1 - h_2\right|^2\left[N_0 + \sum_{k=1}^{L}\sqrt{E_{ik}}\left|g_k\right|^2\right]}}\right),$$

$$P_e = Q\left(\sqrt{\frac{E_s\left|h_1 - h_2\right|^2}{2\left[N_0 + \sum_{k=1}^{L}E_{ik}\left|g_k\right|^2\right]}}\right). \tag{3.6}$$

Using $(12-17)$ of [44], (3.6) can be written as

$$P_e = Q\left(\sqrt{\frac{E_s\left|h_1 - h_2\right|^2}{2\left[N_0 + \sum_{k=1}^{L}E_k\right]}}\right),$$

$$P_e = Q\left(\sqrt{\frac{\frac{E_s}{2N_0}\left|h_1 - h_2\right|^2}{1 + \sum_{k=1}^{L}\frac{E_k}{N_0}}}\right) = Q\left(\sqrt{\frac{\frac{E_s}{2N_0}\left|H\right|^2}{1 + \sum_{k=1}^{L}\frac{E_k}{N_0}}}\right), \tag{3.7}$$

where, $H = h_1 - h_2$, (3.7) can further be expressed in terms of γ_e

$$P_e = Q\left(\sqrt{\gamma_e}\right), \tag{3.8}$$

where, $\gamma_e = \frac{\frac{E_s}{2N_0}|h_1-h_2|^2}{1+\sum_{k=1}^{L}\frac{E_k}{N_0}}$, and Q is defined in (2.9).

Probability Density Function (PDF)

Since H is a circularly symmetric Gaussian distributed and γ_e is Rayleigh distributed, similar to (2.16), the PDF can be written as

$$f_{\gamma e}\left(\gamma_e\right) = \frac{1}{\bar{\gamma_e}}\exp\left(\frac{-\gamma_e}{\bar{\gamma_e}}\right), \tag{3.9}$$

where, $\bar{\gamma_e} = \mathbb{E}\left(\gamma_e\right) = \mathbb{E}\left(\frac{\frac{E_s}{2N_0}|h_1-h_2|^2}{1+\sum_{k=1}^{L}\frac{E_k}{N_0}}\right)$.

Average Bit Error Rate (ABER)

The ABER can be computed by averaging CBER in (3.8) over the Probability Density Function (PDF) of γ_e given in (3.9) .

$$ABER = \int_0^\infty P_e\left(\gamma_e\right) f_{\gamma e}\left(\gamma_e\right) d\gamma_e. \tag{3.10}$$

Therefore, placing (3.8) and (3.9) in (3.10), ABER can be written as

$$ABER = \int_0^\infty Q\left(\sqrt{\gamma_e}\right) \frac{1}{\bar{\gamma}_e} \exp\left(\frac{-\gamma_e}{\bar{\gamma}_e}\right) d\gamma_e. \tag{3.11}$$

After solving the integral, ABER can be computed as

$$ABER = \frac{1}{2}\left(1 - \sqrt{\frac{\bar{\gamma}_e/2}{1+\bar{\gamma}_e/2}}\right),$$
$$ABER = \frac{1}{2}\left(1 - \sqrt{\frac{\bar{\gamma}_e}{2+\bar{\gamma}_e}}\right). \tag{3.12}$$

Simulation Results

In this section, MATLAB simulated results for ABER performance of SSK with perfect channel estimation and in the presence of CCI for the single receiving antenna are presented. For the simulation, at least 10^6 channel realizations are considered over the uncorrelated Rayleigh fading channel. Furthermore, simulated results are compared with the analytically derived result to show the accuracy of the analytical result.

Figure 3.7, shows the ABER versus SNR graph for single receiving antenna. This graph has been plotted by varying the number of interferers, ranging from L = 0 (no interference) to L = 5, in order to briefly analyze the effect of an increase in CCI on performance of the system.

It can be seen in the figure that, with the increase in the number of interferers, there is an enhancement in ABER, i.e., as interfering users are increasing, the performance of the system is degrading. When there is no interference (L = 0), ABER of 10^{-2} is observed at 17dB SNR. Whereas, when L = 1, ABER of 10^{-2} is observed at 19dB SNR, which shows the loss by 2dB. Furthermore, in the case of L = 2 the ABER of 10^{-2} is achieved at 29dB SNR, showing the loss of 12dB as compared to ABER with no interference. Also, it can be clearly seen in the figure that for all the cases when number of interferers are more than 2, i.e., L = 3, 4 or 5, the ABER of 10^{-2} cannot be achieved till 30dB of SNR.

Figure 3.7 also illustrates that with the increase in SNR there is a rise in the performance,

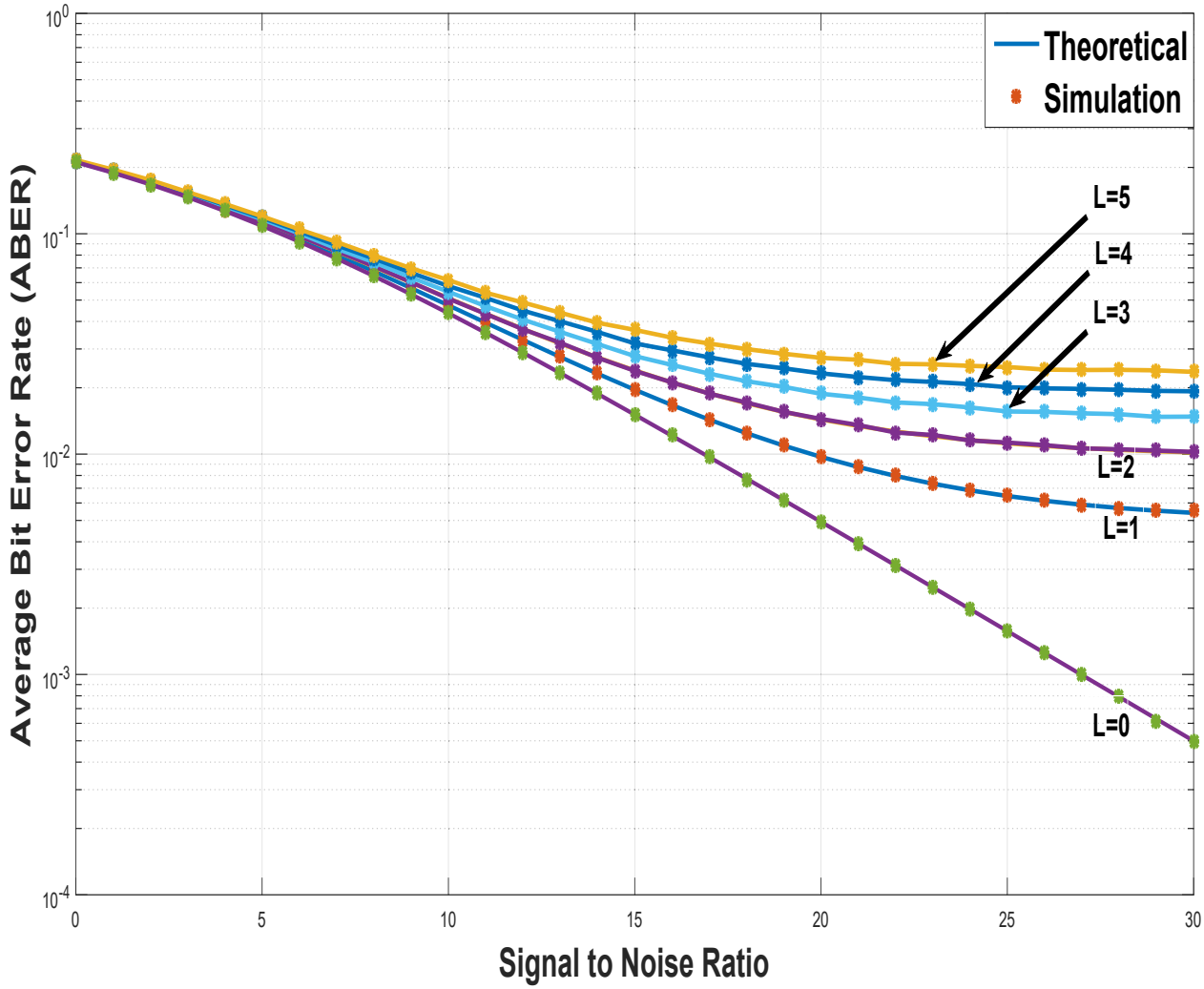

Figure 3.7: Analytical, Simulation results of ABER versus SNR for SSK system with multiple interferers over uncorrelated Rayleigh fading channels

and at low SNR the performance for L = 1 to L = 5 is approximately equal. Moreover, with the simultaneous increase in SNR and interference, there occurs an error floor, which can be explained as when energy of desired signal and energy of the interference both increase simultaneously, the ABER gets independent of both, as energy of the desired signal and energy of the interference cancel out each other.

3.3.2 Asymptotic Analysis in Presence of Uncorrelated Rayleigh Fading Channels

Using (3.9), the PDF can be written as

$$f_{\gamma_e}(\gamma_e) = \frac{1}{\bar{\gamma_e}} \exp\left(\frac{-\gamma_e}{\bar{\gamma_e}}\right),$$

where $\bar{\gamma_e} = \mathbb{E}(\gamma_e) = \mathbb{E}\left(\frac{\frac{E_s}{2N_0}|h_1 - h_2|^2}{1+\sum_{k=1}^{L}\frac{E_k}{N_0}}\right)$.

Applying the Taylor series expansion, PDF can be written as

$$f_{\gamma_e}(\gamma_e) = \frac{1}{\frac{\frac{E_s}{N_0}}{1+\sum_{k=1}^{L} E_k}} + HOT, \tag{3.13}$$

where HOT refers to the Higher Order Terms.

Asymptotic ABER

Using the equation of ABER given in (3.10)

$$ABER = \int_0^\infty P_e(\gamma_e) f_{\gamma_e}(\gamma_e) d\gamma_e,$$

where $P_e(\gamma_e)$ is given in (3.8) and $f_{\gamma_e}(\gamma_e)$ is given in (3.13). Hence, neglecting the Higher Order Terms of (3.13), asymptotic ABER can be written as

$$AABER \simeq \int_0^\infty Q(\sqrt{\gamma_e}) \frac{1}{\bar{\gamma_e}} d\gamma_e, \tag{3.14}$$

$$AABER \simeq \frac{1}{\bar{\gamma_e}} \int_0^\infty Q(\sqrt{\gamma_e}) d\gamma_e.$$

On integrating the above equation asymptotic ABER can be computed as

$$AABER \simeq \frac{1}{2\bar{\gamma_e}} = \frac{1}{2\frac{\frac{E_s}{N_0}}{1+\sum_{k=1}^{L}\frac{E_k}{N_0}}} \tag{3.15}$$

Simulation Results

In this section, comparison of asymptotic and exact ABER results of the SSK Modulation communication system in presence of CCI is provided.

It can be seen in Fig. 3.8 that asymptotic and exact results overlap each other or both are exactly the same in the region of higher SNR. The results have been presented by varying the number of cochannel interferers for the system with single receiving antenna.

It can be noticed from the figure that, for L=0, the asymptotic and exact results start overlapping from around SNR = 17dB. Whereas, for L = 1, they start overlapping around SNR= 25dB. However, for L = 3 and L = 4 they do not even overlap at SNR = 30dB, which shows that the accuracy of asymptotic result keeps on decreasing with increase in interference; i.e., the asymptotic result loses its tightness with the increase in number of interfering users.

3.3.3 Exact Analysis in Presence of Correlated Rayleigh Fading Channels

Using (3.6) and (3.7), CBER can be written as

$$P_e = Q\left(\sqrt{\frac{\frac{E_s}{2N_0}\left|h_1 - h_2\right|^2}{1+\sum_{k=1}^{L}\frac{E_k}{N_0}}}\right) = Q\left(\sqrt{\frac{\frac{E_s}{2N_0}\left|H\right|^2}{1+\sum_{k=1}^{L}\frac{E_k}{N_0}}}\right),$$

where, $H = h_1 - h_2$, similar to (3.8) the above Eqn. can further be expressed in terms of γ_{ec}.

$$P_e = Q\left(\sqrt{\gamma_{ec}}\right),$$

where, $\gamma_{ec} = \frac{\frac{E_s}{2N_0}|h_1-h_2|^2}{1+\sum_{k=1}^{L}\frac{E_k}{N_0}}$ and Q function is given in (2.9).

Using (3.9), PDF can be written as

$$f_{\gamma_{ec}}\left(\gamma_{ec}\right) = \frac{1}{\bar{\gamma_{ec}}}\exp\left(\frac{-\gamma_{ec}}{\bar{\gamma_{ec}}}\right),$$

where, $\bar{\gamma_{ec}} = \mathbb{E}\left(\gamma_{ec}\right) = \mathbb{E}\left(\frac{\frac{E_s}{2N_0}|h_1-h_2|^2}{1+\sum_{k=1}^{L}\frac{E_k}{N_0}}\right) = \frac{\frac{E_s\sigma^2(1\ \ \rho)}{N_0}}{1+L\frac{E_k}{N_0}}$,

where, σ^2 is the variance of each fading channel = 1 and ρ is the correlation coefficient between fading channels.

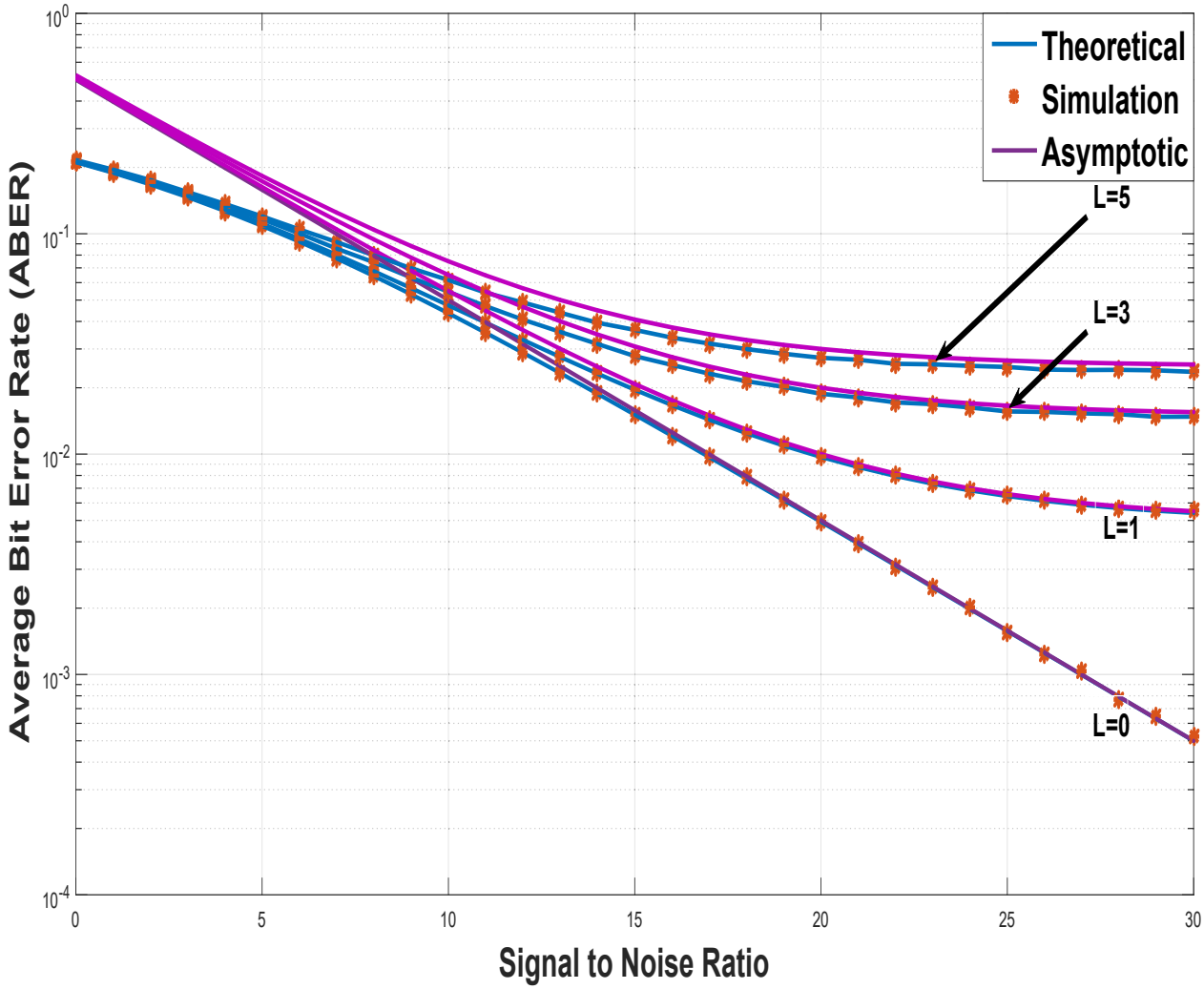

Figure 3.8: Comparison of Asymptotic and Exact results of ABER v/s SNR for SSK system in presence of CCI over Uncorrelated Rayleigh fading channels

Average Bit Error Rate (ABER)

ABER can be written as in eqn 3.10 and 3.11

$$ABER = \int_0^\infty P_e\left(\gamma_{ec}\right) f_{\gamma_{ec}}\left(\gamma_{ec}\right) d\gamma_{ec},$$
$$ABER = \int_0^\infty Q\left(\sqrt{\gamma_{ec}}\right) \frac{1}{\bar{\gamma_{ec}}} \exp\left(\frac{-\gamma_{ec}}{\bar{\gamma_{ec}}}\right) d\gamma_{ec}.$$

ABER can be computed as

$$ABER = \frac{1}{2}\left(1 - \sqrt{\frac{\bar{\gamma_{ec}}/2}{1+\bar{\gamma_{ec}}/2}}\right) = \frac{1}{2}\left(1 - \sqrt{\frac{\bar{\gamma_{ec}}}{2+\bar{\gamma_{ec}}}}\right), \tag{3.16}$$

where, $\bar{\gamma ec} = \frac{\frac{E_s(1\ \ \rho)}{N_0}}{1+L\frac{E_k}{N_0}}$.

Simulation Results

In this section, MATLAB simulated results for ABER in the presence of correlated Rayleigh fading channels have been illustrated. Results are provided by varying the value of correlation coefficient, for $\rho = 0$, 0.5, and 0.9, along with varying the number of cochannel interferers for L = 0, 1, and 5.

It can be observed from the figure 3.9 that correlation coefficient and number of cochannel interferers both are inversely proportional to the performance of the system. The increase in both degrades the performance of the system, resulting in an increase of ABER.

3.4 Performance Analysis for Multiple Receiving Antenna with Perfect CSI and Multiple Co-channel interferers

3.4.1 Exact Analysis in Presence of Uncorrelated Rayleigh Fading Channels

Transmission and Reception

The Received signal at receiving end can be written as

$$y_r = \sqrt{E_s} h_{r,t} + \sum_{k=1}^{L} \sqrt{E_{ik}} g_k + w_r, \qquad t = 1, 2, \tag{3.17}$$

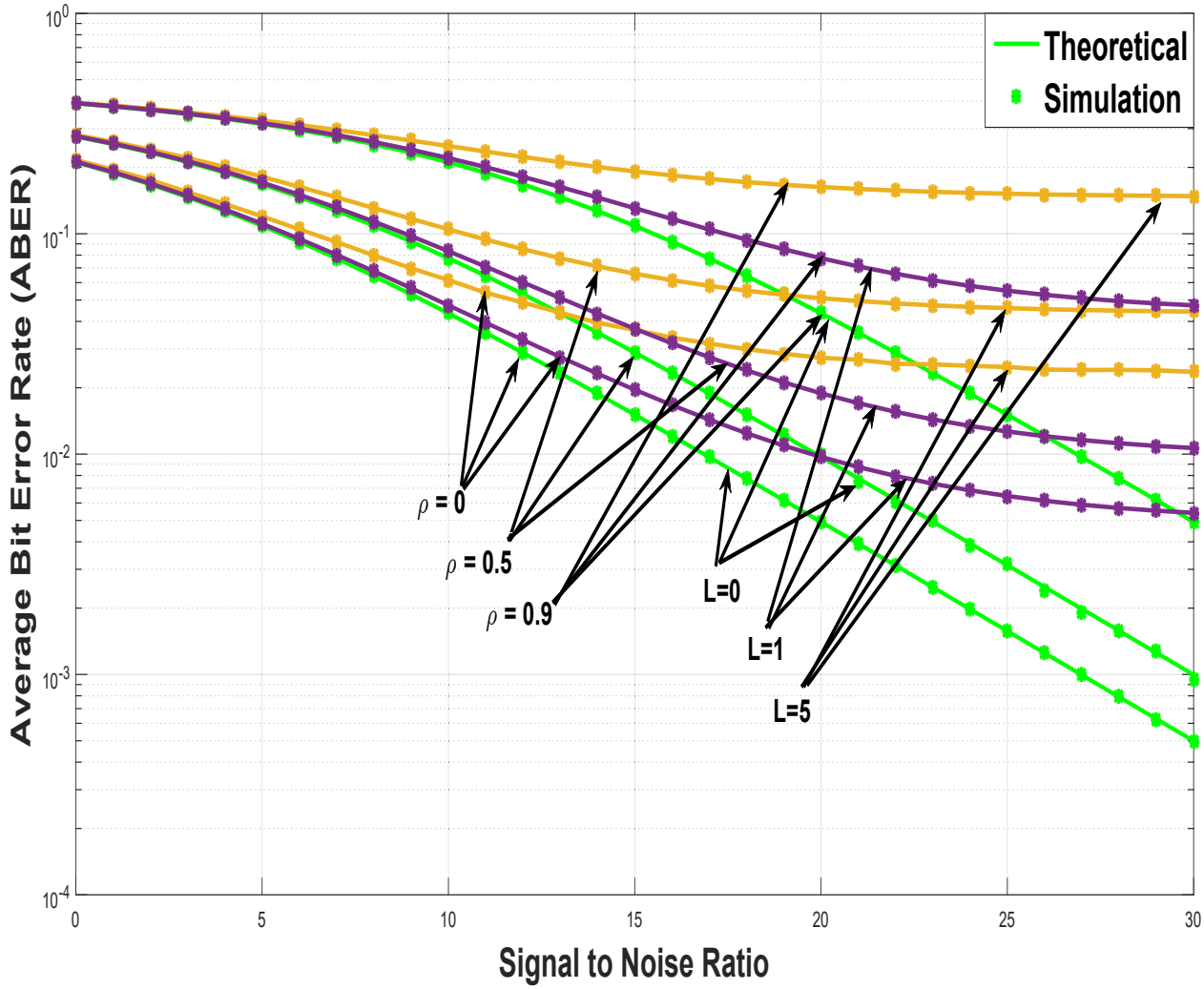

Figure 3.9: Analytical, Simulation results of ABER v/s SNR for SSK system with CCI over Correlated Rayleigh fading channels

where, $\sqrt{E_s}$ is the energy of desired signal, $\sqrt{E_{ik}}$ is the energy of k^{th} interfering user, $h_{r,t}$ and g_k are the complex Gaussian Rayleigh fading channel of activated t^{th} transmitting and r^{th} receiving antenna, and the k_{th} interfering user with mean zero and variance 1, $h_{r,t} \sim \mathcal{CN}(0,1)$, $g_k \sim \mathcal{CN}(0,1)$ and w is the complex Gaussian white noise, with mean zero and variance N_0, $w \sim \mathcal{CN}(0, N_0)$. Both $h_{r,t}$ and g_k are considered mutually independent of each other. It has been assumed that, there is perfect channel estimation at the receiver.

In the system model, two transmitting antennas and N_r receiving antennas are considered. Thus, to transmit symbol 0, Tx1 is activated and to transmit symbol 1, Tx2 is activated. On the activation of Tx1 received signal can be written as, $y_{r,1} = \sqrt{E_s}h_{r,1} + \sum_{k=1}^{L}\sqrt{E_{ik}}g_k + w_r$ and on the activation of Tx2 received signal can be written as, $y_{r,2} = \sqrt{E_s}h_{r,2} + \sum_{k=1}^{L}\sqrt{E_{ik}}g_k + w_r$ is our received signal.

Table 3.2: SSK Mapping for multiple receiving antennas with CCI

symbol	Tx activated	Received Signal at r^{th} Receive Antenna
0	1	$y_{r,1} = \sqrt{E_s}h_{r,1} + \sum_{k=1}^{L}\sqrt{E_{ik}}g_k + w_r$
1	2	$y_{r,2} = \sqrt{E_s}h_{r,2} + \sum_{k=1}^{L}\sqrt{E_{ik}}g_k + w_r$

Detection

MRC based ML detector used at the receiver is as written below

$$u = arg\min_{t=1,2}\left(\sum_{r=1}^{N_r}\left|y_r - \sqrt{E_s}hr,t\right|^2\right). \tag{3.18}$$

Assuming that the symbol to be transmitted is 0. Therefore, the received signal at r^{th} receive antenna can be written as

$$y_1 = \sqrt{E_s}h_{r,1} + \sum_{k=1}^{L}\sqrt{E_{ik}}g_k + w_r. \tag{3.19}$$

Using ML detection method, error (P_e) is defined as

$$P_e = P_r\left(\sum_{r-1}^{N_r}\left|y_1 - \sqrt{E_s}h_{r,1}\right|^2 > \sum_{r=1}^{N_r}\left|y_1 - \sqrt{E_s}h_{r,2}\right|\right), \tag{3.20}$$

$$P_e = P_r\left(\sum_{r=1}^{N_r}\left(2\sqrt{E_s}\Re\left(h_{r,1}-h_{r,2}\right)w^* + \left(h_{r,1}-h_{r,2}\right)\sum_{k=1}^{L}\sqrt{E_{ik}}g_k^*\right) > \sum_{r=1}^{N_r}\left|\sqrt{E_s}\left(h_{r,1}-h_{r,2}\right)\right|^2\right),$$

$$P_e = P_r\left(\sum_{r=1}^{N_r}\left|\sqrt{E_s}\left(h_{r,1}-h_{r,2}\right)\right|^2 < \hat{w}\right), \tag{3.21}$$

where, $\hat{w} = \sum_{r=1}^{N_r}\left(2\sqrt{E_s}\Re\left(h_{r,1}-h_{r,2}\right)w^* + \left(h_{r,1}-h_{r,2}\right)\sum_{k=1}^{L}\sqrt{E_{ik}}g_k^*\right)$.

The variance of $\hat{w}$ can be computed as : $\sigma_w^2 = \mathbb{E}\left(\hat{w}^2\right)$, where $\mathbb{E}$ is the Expectation operator. Therefore,

$$\sigma_n^2 = 4E_s\sum_{r=1}^{N_r}\left|h_{r,1}-h_{r,2}\right|^2\left[\frac{N_0}{2} + \sum_{k=1}^{L}\frac{\sqrt{E_{ik}}\left|g_k\right|^2}{2}\right],$$

$$\sigma_n^2 = 2E_s\left|h_1-h_2\right|^2\left[N_0 + \sum_{k=1}^{L}\sqrt{E_{ik}}\left|g_k\right|^2\right].$$

Hence, using (2.20) CBER can be written as

$$P_e = Q\left(\sum_{r=1}^{N_r}\frac{\left|\sqrt{E_s}\left(h_{r,1}-h_{r,2}\right)\right|^2}{\sqrt{2E_s\left|h_{r,1}-h_{r,2}\right|^2\left[N_0+\sum_{k=1}^{L}\sqrt{E_{ik}}\left|g_k\right|^2\right]}}\right),$$

$$P_e = Q\left(\sum_{r=1}^{N_r}\sqrt{\frac{E_s\left|h_{r,1}-h_{r,2}\right|^2}{2\left[N_0+\sum_{k=1}^{L}E_{ik}\left|g_k\right|^2\right]}}\right). \tag{3.22}$$

Using the similar process as used to obtain (3.7) , (3.19) can be written as

$$P_e = Q\left(\sqrt{\frac{\sum_{r=1}^{N_r}E_s\left|h_{r,1}-h_{r,2}\right|^2}{2\left[N_0+\sum_{k=1}^{L}E_k\right]}}\right),$$

$$P_e = Q\left(\sqrt{\frac{\sum_{r=1}^{N_r}\frac{E_s}{2N_0}\left|h_{r,1}-h_{r,2}\right|^2}{1+\sum_{k=1}^{L}\frac{E_k}{N_0}}}\right). \tag{3.23}$$

(3.23) can further be expressed in terms of γ_e as

$$P_e = Q\left(\sqrt{\gamma_e}\right), \tag{3.24}$$

where, $\gamma_e = \frac{\sum_{r=1}^{N_r} \frac{E_s}{2N_0} |h_{r,1} - h_{r,2}|^2}{1+\sum_{k=1}^{L} \frac{E_k}{N_0}}$, and Q is defined in (2.9).

Probability Density Function (PDF)

Similar to (2.36), PDF of γ_e can be written as

$$f_{\gamma_e}(\gamma_e) = \frac{1}{(N_r-1)!} \left(\frac{1}{\bar{\gamma_e}}\right)^{N_r} \gamma_e^{N_r-1} \exp\left(\frac{-\gamma_e}{\bar{\gamma_e}}\right), \tag{3.25}$$

where, $\bar{\gamma_e} = \mathbb{E}(\gamma_e) = \mathbb{E}\left(\frac{\sum_{r=1}^{N_r} \frac{E_s}{2N_0} |h_{r,1} - h_{r,2}|^2}{1+\sum_{k=1}^{L} \frac{E_k}{N_0}}\right)$.

Average Bit Error Rate (ABER)

The ABER can be computed by averaging CBER in (3.24) over the PDF of γ_e given in (3.25).

Hence, the ABER can be written as in (2.17). Therefore, substituting (3.24) and (3.25) in (2.17)

$$ABER = \int_0^\infty Q(\sqrt{\gamma_e}) \frac{1}{(N_r-1)!} \left(\frac{1}{\bar{\gamma_e}}\right)^{N_r} \gamma_e^{N_r-1} \exp\left(\frac{-\gamma_e}{\bar{\gamma_e}}\right) d\gamma_e. \tag{3.26}$$

The above equation can further be computed as

$$ABER = \gamma_a^{N_r} \sum_{k=0}^{N_r-1} \binom{N_r-1+k}{k} [1-\gamma_a]^k, \tag{3.27}$$

where, $\gamma_a = \frac{1}{2}\left(1 - \sqrt{\frac{\bar{\gamma_c}/2}{1+\bar{\gamma_c}/2}}\right) = \frac{1}{2}\left(1 - \sqrt{\frac{\bar{\gamma_c}}{2+\bar{\gamma_c}}}\right)$,
where, $\bar{\gamma_c} = \frac{\bar{\gamma_e}}{N_r}$.

Simulation Results

In this section, MATLAB simulated results for ABER performance of SSK with the perfect channel estimation and in the presence of CCI for multiple receiving antennas are presented. In this simulation at least 10^6 channel realizations have been considered over the uncorrelated Rayleigh fading channels. Furthermore, simulation results are compared with the mathematically derived analytical results.

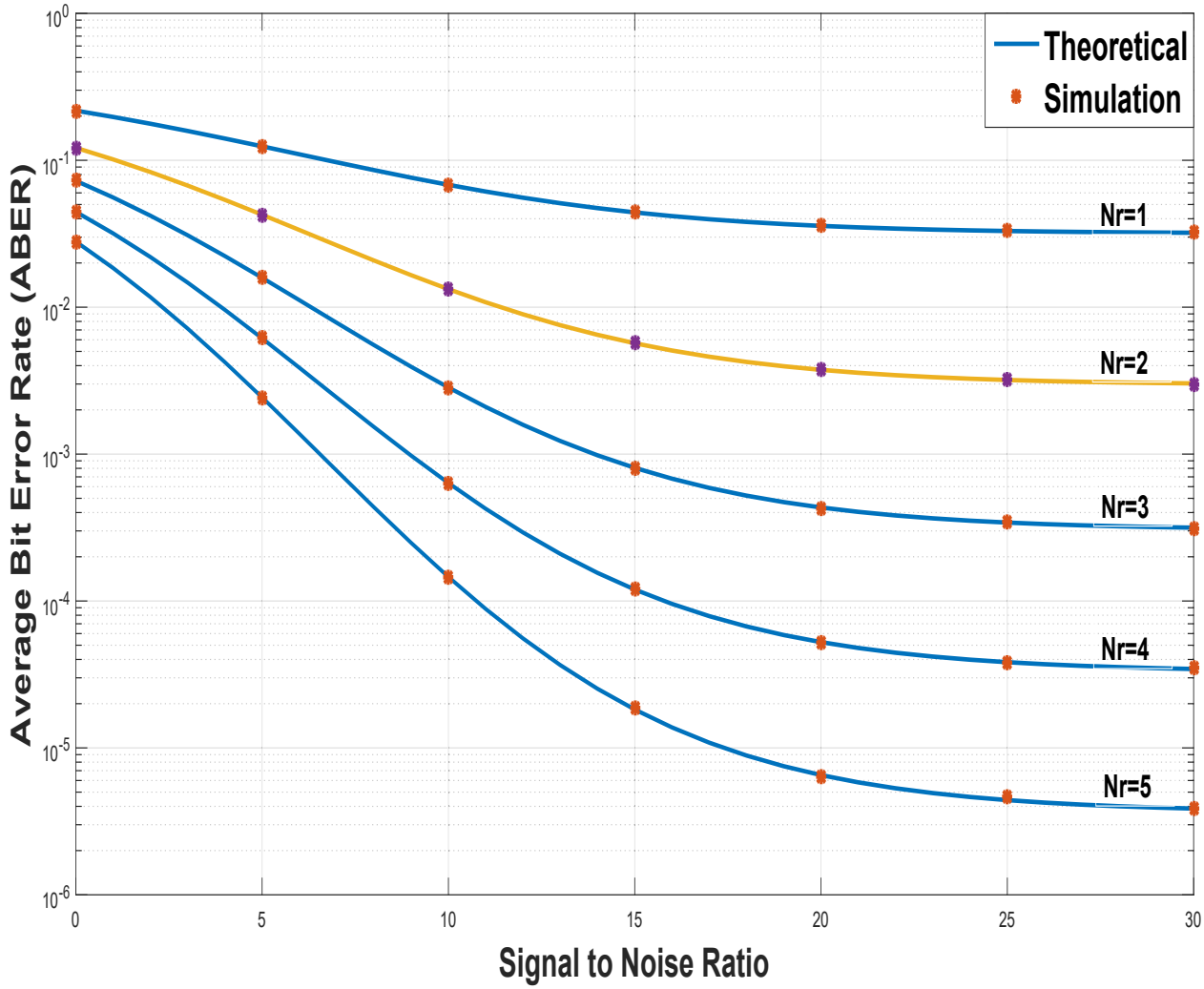

Figure 3.10: Analytical, Simulation results of ABER versus SNR for SSK system with multiple interferers over uncorrelated Rayleigh fading channels

Figure 3.10 shows the ABER versus SNR graph, plotted for different numbers of receiving antennas ($N_r = 1, 2, 3, 4, 5$). In this simulation, each of the received signals is subjected to 7 equal power co-channel interferers. This graph has been plotted for different values of SNR ranging from 0dB to 30dB. This figure has been plotted to study the effect of receive diversity in the presence of a fixed number of interfering users on the performance of the system.

It can be seen in the figure that, with the increase in the number of receiving antennas, there is a decrease in ABER, which indicates the increase in performance. However, due to the presence of interference, performance cannot be as good as in the absence of interference. It can be seen in the figure that, at SNR = 0dB, there is a significantly smaller gap between the curves for different number of receiving antennas; however, as the SNR goes on increasing, the gap between curves also goes on increasing. Due to this it can be stated that performance is increased with the increase in number of antennas and SNR, while keeping interference constant.

Also, it can be noted from the figure 3.10 that, for $N_r = 1$ in presence of 7 co-channel interferers ABER of $10^{-1.6}$ is reached at SNR of 20dB and for $N_r = 2$, ABER of $10^{-2.6}$ is reached at SNR = 20dB. Curve for $N_r = 3$ shows that the ABER of $10^{-3.6}$ is obtained at SNR = 20dB. Moreover with $N_r = 4$ at SNR = 20dB, ABER = $10^{-4.5}$ is measured. Furthermore with $N_r = 5$ at SNR = 20dB, ABER = $10^{-5.4}$ is observed. By comparing all the curves it is noticed that with the increase of 1 antenna when SNR and number of co-channel interferers with same power are kept constant, there is an approximately equal increase in performance or decrease in ABER.

It can also be noticed from the figure that, due to the high interference energy, there is an error floor at high SNR.

3.4.2 Asymptotic Analysis in Presence of Uncorrelation Rayleigh Fading Channels

Using the CBER given in 3.23

$$P_e = Q\left(\sqrt{\frac{\sum_{r=1}^{N_r} \frac{E_s}{2N_0} \left|h_{r,1} - h_{r,2}\right|^2}{1 + \sum_{k=1}^{L} \frac{E_k}{N_0}}}\right).$$

Similar to (3.24), above Eqn. can further be expressed in terms of γ_e as

$$P_e = Q\left(\sqrt{\gamma_e}\right), \tag{3.28}$$

where, $\gamma_e = \frac{\sum_{r=1}^{N_r} \frac{E_s}{2N_0} |h_{r,1} - h_{r,2}|^2}{1+\sum_{k=1}^{L} \frac{E_k}{N_0}}$.

Using, PDF given in (3.25)

$$f_{\gamma_e}(\gamma_e) = \frac{1}{(N_r - 1)!} \left(\frac{1}{\bar{\gamma_e}}\right)^{N_r} \gamma_e^{N_r - 1} \exp\left(\frac{-\gamma_e}{\bar{\gamma_e}}\right),$$

where, $\bar{\gamma_e} = \mathbb{E}(\gamma_e) = \mathbb{E}\left(\frac{\sum_{r=1}^{N_r} \frac{E_s}{2N_0} |h_{r,1} - h_{r,2}|^2}{1+\sum_{k=1}^{L} \frac{E_k}{N_0}}\right)$.

Applying Taylor Series to above written equation, the PDF can be re-written as

$$f_{\gamma_e}(\gamma_e) = \frac{1}{(N_r - 1)!} \left(\frac{1}{\bar{\gamma_e}}\right)^{N_r} \gamma_e^{N_r - 1} + H.O.T, \tag{3.29}$$

where, H.O.T refers to Higher Order Terms.

Asymptotic ABER

Substituting (3.28) and (3.29) in equation 2.17, the asymptotic ABER can be written as

$$AABER = \int_0^{\infty} Q\left(\sqrt{\gamma_e}\right) \frac{1}{(N_r - 1)!} \left(\frac{1}{\bar{\gamma_e}}\right)^{N_r} \gamma_e^{N_r - 1} d\gamma_e.$$

The above written equation of AABER can further be computed as

$$AABER = \frac{1}{N_r!} \left(\frac{1}{\bar{\gamma_e}}\right)^{N_r} \frac{2^{(N_r-1)}\Gamma(N_r + 0.5)}{\sqrt{\pi}} = \left(\frac{1}{\bar{\gamma}}\right)^{N_r} C, \tag{3.30}$$

where C is a constant dependent on the diversity order at receiver, Beign a constant relying on the number of receiving antennas N_r, 2.42 clearly indicates that in the absence of interference, the diversity order equal to the number of receiving antennas N_r can be obtained. 2.42 also indicates that when interference energy is independent of SNR error floors could be seen, However the Gaussian interference decreases with the increase in SNR, the diversity gain of N_r can be acquired.

Simulation Results

In this section, the comparison of exact and asymptotic ABER results for a different number of receiving antennas ((N_r)= 1,2,3,4 and 5) has been provided. It is clearly visible from Fig. 3.11 that at high SNR, as the value of N_r is increasing i.e., as the number of receiving antennas in the system are increasing, the gap between, asymptotic and exact results is also increasing. It is illustrated in the figure that, for $N_r = 1$ at SNR = 30dB there is very little gap between asymptotic and exact results or they are almost similar. However, as the N_r is increasing the gap between both the curves is increasing, as seen in $N_r = 5$ where the gap at SNR = 30dB is most among all shown. This clearly indicates that as the number of receiving antennas increases, the asymptotic results loses its tightness.

3.4.3 Exact Analysis in Presence of Correlated Rayleigh Fading Channels

Using 3.23, CBER can be written as

$$P_e = Q\left(\sqrt{\frac{\sum_{r=1}^{N_r} \frac{E_s}{2N_0} \left|h_{r,1} - h_{r,2}\right|^2}{1 + \sum_{k=1}^{L} \frac{E_k}{N_0}}}\right). \tag{3.31}$$

Similar to (3.24), the above Eqn. can be represented in terms of γ_{ec} as

$$P_e = Q\left(\sqrt{\gamma_{ec}}\right), \tag{3.32}$$

where, $\gamma_{ec} = \frac{\sum_{r=1}^{N_r} \frac{E_s}{2N_0} |h_{r,1} - h_{r,2}|^2}{1 + \sum_{k=1}^{L} \frac{E_k}{N_0}}$.

Using (3.25), the PDF can be written as

$$f_{\gamma_{ec}}\left(\gamma_{ec}\right) = \frac{1}{(N_r - 1)!} \left(\frac{1}{\bar{\gamma_{ec}}}\right)^{N_r} \gamma_{ec}^{N_r - 1} \exp\left(\frac{-\gamma_{ec}}{\bar{\gamma_{ec}}}\right), \tag{3.33}$$

where, $\bar{\gamma_{ec}} = \mathbb{E}\left(\gamma_{ec}\right) = \mathbb{E}\left(\frac{\sum_{r=1}^{N_r} \frac{E_s}{2N_0} |h_{r,1} - h_{r,2}|^2}{1 + \sum_{k=1}^{L} \frac{E_k}{N_0}}\right) = \frac{\frac{N_r E_s \sigma^2 (1 \quad \rho)}{N_0}}{1 + L\frac{E_k}{N_0}}$,
where, N_r is the number of receiving antennas, σ^2 is the variance of each fading channel =1, and ρ is the correlation coefficient between fading channels.

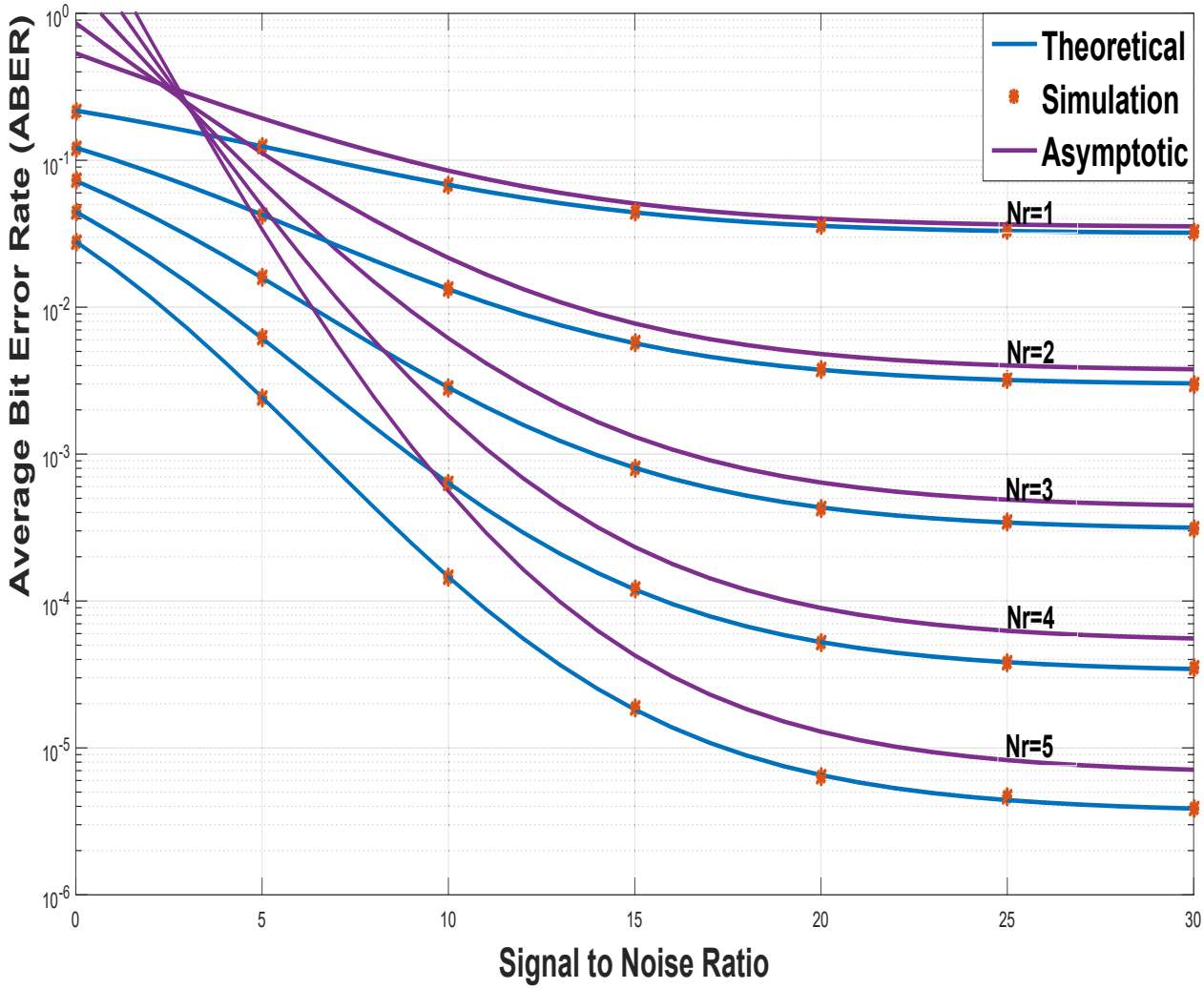

Figure 3.11: Comparison of Asymptotic and Exact results of ABER versus SNR for SSK system in presence of CCI over Uncorrelated Rayleigh fading channels

Average Bit Error Rate (ABER)

Hence, using 2.17 an similar to 3.26 the ABER can be computed as

$$ABER = \int_0^\infty Q\left(\sqrt{\gamma_{ec}}\right) \frac{1}{(N_r-1)!} \left(\frac{1}{\bar{\gamma_{ec}}}\right)^{N_r} \gamma_{ec}^{N_r-1} \exp\left(\frac{-\gamma_{ec}}{\bar{\gamma_{ec}}}\right) d\gamma_{ec}, \tag{3.34}$$

$$ABER = \gamma_{ac}^{N_r} \sum_{k=0}^{N_r-1} \binom{N_r-1+k}{k} \left[1-\gamma_{ac}\right]^k, \tag{3.35}$$

where, $\gamma_{ac} = \frac{1}{2}\left(1-\sqrt{\frac{\bar{\gamma_c}/2}{1+\bar{\gamma_c}/2}}\right) = \frac{1}{2}\left(1-\sqrt{\frac{\bar{\gamma_c}}{2+\bar{\gamma_c}}}\right)$,

where, $\bar{\gamma_c} = \frac{\bar{\gamma_{ec}}}{N_r}$ and $\bar{\gamma_{ec}} = \frac{\frac{N_r E_s(1\ \ \rho)}{N_0}}{1+L\frac{E_k}{N_0}}$.

Simulation Results

In this section, MATLAB based plot showing the analytical and simulation results for exact ABER in the presence of correlated Rayleigh fading channels have been provided. Results for a different number of receiving antennas (N_r = 1, 3, and 5), varying the values of correlation coefficient (ρ = 0, 0.5, and 0.9) are provided. Moreover, it has been assumed that all the desired signals are interfered by 7 (L = 7) equal power interferers.

Fig. 3.12 shows that the value of correlation coefficient and ABER are proportional i.e with an increase in one, there is an increase in other or vice-versa (enhancement in ABER shows degradation in performance). Whereas, the number of receiving antennas and ABER are inversely proportional; i.e., increase in one degrades other. Among all the systems shown in Fig. 3.12, system with $N_r = 5$ and $\rho = 0$ gives the best performance, but the system with $N_r = 1$ and $\rho = 0.9$ gives the worst performance among all the systems plotted in the figure.

The figure also demonstrates that the effect of correlation increases with the number of receiving antennas in the system. For example, in the case of $N_r = 1$ the gap between curves for ρ = 0, 0.5 and 0.9, which is less compared to the gap for $N_r = 3$ and the gap is most pronounced for $N_r = 5$. Therefore, it can be said that the effect of correlation increases with an increase in the number of receiving antennas.

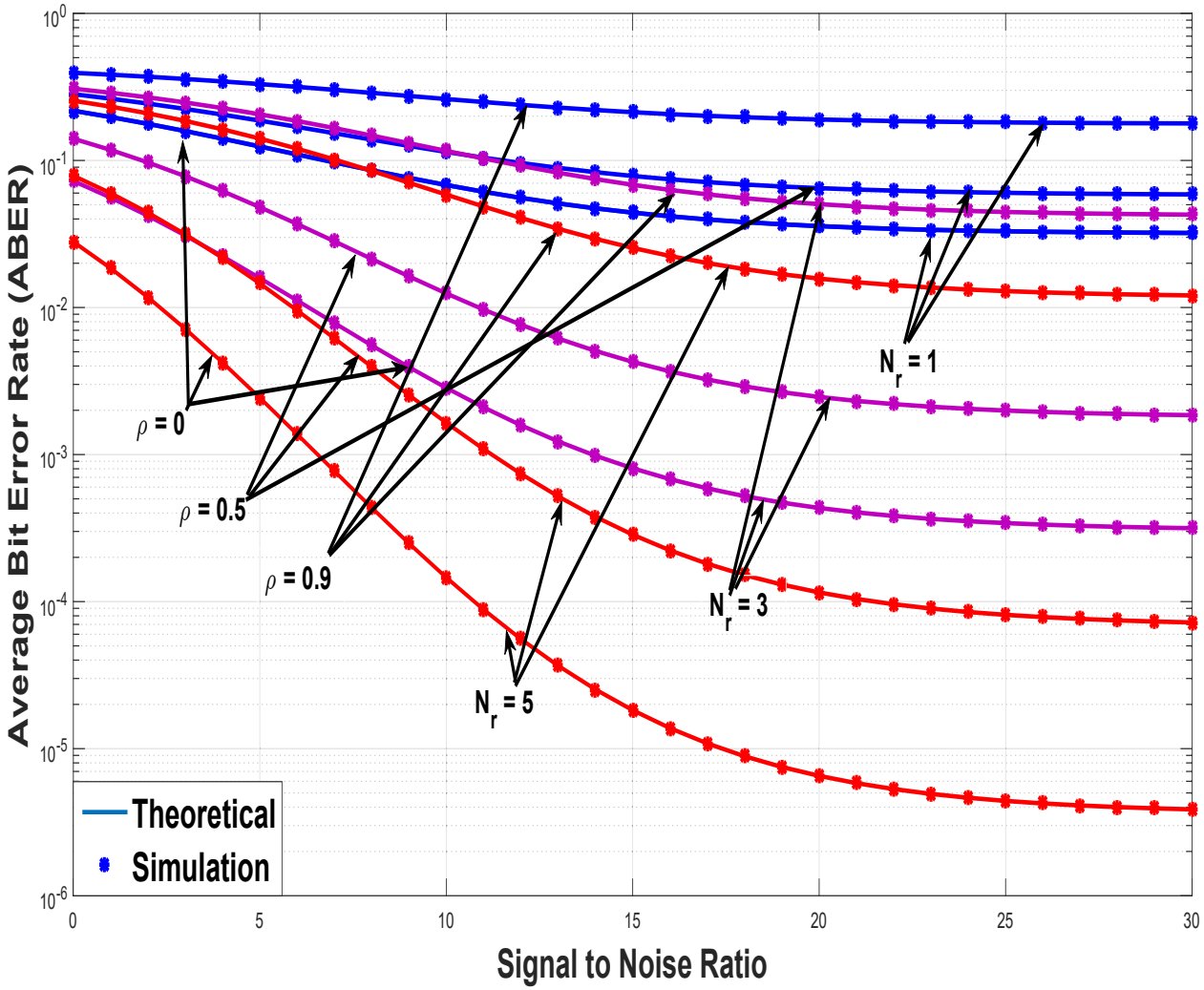

Figure 3.12: Analytical, Simulation results of ABER versus SNR for SSK system in presence of interference over Correlated Rayleigh fading channels

Chapter 4

Conclusions and Future Applications

4.1 Conclusions

In this thesis, the Average Bit Error Rate, as the performance parameter for Space Shift Keying Modulation in absence and presence of Co-Channel Interference has been studied, therefore, studying the effects of Co-Channel Interference on Space Shift Keying Modulation system. The analysis has been studied twice considering Correlated and Uncorrelated Rayleigh fading channels.

In the first section of Chapter 2, the performance of Space Shift Keying Modulation in the absence of Co-Channel Interference was studied, assuming that there is a perfect channel estimation available at the receiver, and the noise at receiving antenna is Additive White Gaussian Noise. The exact mathematical expression for Average Bit Error Rate and the expression for asymptotic Average Bit Error Rate for Binary Phase Shift Keying signal over Rayleigh fading channels, using the Maximum Likelihood detection method has been derived. The expression for exact Average Bit Error Rate has been derived twice, considering Correlated and Uncorrelated Rayleigh fading channels. In this section, a system with two transmitting antennas and a single receiving antenna has been considered for the analysis. Later, MATLAB simulated results were provided to support the accuracy of theoretically derived results for the exact ABER in the presence of Correlated and Uncorrelated Rayleigh fading channels. It has been observed that the asymptotic and exact results are exactly the same at high SNR. Correlation in the fading

channels degrades the performance of a system; the more correlation between fading channels, the more degradation occurs in performance (increase in Average Bit Error Rate).

In the second section of Chapter 2, an exact analytical expression for Average Bit Error Rate and expression for asymptotic Average Bit Error Rate of SSK Modulation communication system has been derived. The expression for the exact Average Bit Error Rate has been derived twice, considering Correlated and Uncorrelated Rayleigh fading channels. In this section, the communication system with two transmitting and an arbitrary number of receiving antennas have been considered for the transmission and reception of Binary Phase Shift Keying signals. MATLAB simulations for ABER in the presence of Correlated and Uncorrelated Rayleigh fading channels were performed with multiple receiving antennas ranging from $N_r = 1$ to $N_r = 5$. In this analysis, the Maximum Ratio Combining based Maximum Likelihood detection technique has been used. On comparing the results, it has been observed that there is a significant gain in Signal to Noise Ratio with an increase in receive diversity. Also, the asymptotic result loses its tightness with the increase in receive diversity and the effect of correlation enhances with an increase in the number of antennas at receiver.

Chapter 3 provides the analysis for the exact Average Bit Error Rate and asymptotic performance of Space Shift Keying Modulation over the Rayleigh fading Channels for Binary Phase Shift Keying signal in the presence of multiple co-channel interferers and Additive White Gaussian Noise. It has been assumed that there is perfect Channel State Information available at the receiving end of the communication system. The exact Average Bit Error Rate expression has been derived twice, considering Correlated and Uncorrelated Rayleigh fading channels. To obtain the exact analytical expressions, it was considered that the decision variable is conditioned only on the fading channel of active or desired user [44] and the Gaussian distribution of Interference-plus-Noise Ratio was found by conditioning only on the fading channel of the desired user, resulting in the exact expression of Conditional Bit Error Rate and Average Bit Error Rate [44].

In the first section of Chapter 3, the performance was analyzed, considering two transmitting antennas and single receiving antenna; MATLAB simulated results have also been provided as proof of the accuracy of theoretical result for exact Average Bit Error Rate in presence of Correlated and Uncorrelated Rayleigh fading channels. The results were compared, varying the number of Co-Channel Interferers attacking the desired received signal. Interfering users have been varied from L=0 (no interference) to L=5 (5 interfering users). From the analysis, it has been observed that there is a significant loss of Signal to Noise Ratio with an increase in Co-Channel Interference. Also, with the enhancement in interference, asymptotic results lose tightness. Moreover, with the simultaneous increase in the energy of desired signal and energy of interfering users, there is an occurrence of an error floor.

In the second section of Chapter 3, Average Bit Error Rate and asymptotic Average Bit Error Rate performance for Space Shift Keying Modulation communication system with two transmitting antennas and Nr (multiple) receiving antennas have been analyzed. The exact analytical expression for Average Bit Error Rate, considering Correlated and Uncorrelated Rayleigh fading channels and expression for asymptotic Average Bit Error Rate considering Uncorrelated Rayleigh fading channels have been derived. Also, MATLAB simulated results were provided in support of mathematically derived theoretical results for Average Bit Error Rate in the presence of Correlated and Uncorrelated Rayleigh fading channels. Later, the results were compared by varying the number of receiving antennas from $N_r = 1$ to $N_r = 5$, when subjected to a fixed number of co-channel interferers. A total of seven users was considered to be interfering with the desired signal. It has been observed that there is an enhancement in performance with the increase in the number of receiving antennas; however, there is a significant degradation in the performance with an increase in the interference. It has also been observed that after the particular range of Signal to Noise Ratio there is an occurrence of error floor, which means that there is no significant increase in performance; i.e., after a particular range of SNR, even upon increasing the SNR, no increase in performance is observed. This is because, when there is a constant increase in the energy of desired signal and the energy of interference, they cancel out each other; therefore, the performance becomes independent of Signal to Noise Ratio as well as

Interference-plus-Noise Ratio. Also, it has been observed that for systems with more receiving antennas, there is more degradation in performance with an increase in the value of correlation coefficient as compared to systems with fewer number of receiving antennas.

4.2 Future Applications

Due to high system capacity, high reliability, achievable energy and high spectral efficiency, Multiple Input Multiple Output systems have attained a huge interest in research for the variety of works such as machine to machine communication (M2M) [59]. Machine to machine communication is referred to as a technique used for direct communication between devices using trillions of intelligent wireless devices with or without human interference. This concept of the machine to machine communication can be used in a variety of applications like Intelligent Transport System, Home Automation, Emergency, and many other industrial applications. Machine to machine communication requires highly reliable and efficient communications for which MIMO and Large MIMO systems are the best options. Other examples of the applications of large MIMO are wireless high definition television, smart phones, laptops, computers, wireless fidelity (wi-fi) and much more.

Bibliography

[1] *http://www.statista.com/statistics/274774/forecast-of-mobile-phone-users-worldwide*, Statista.

[2] Marco Di Renzo et al., "Spatial Modulation for Generalized MIMO: Challenges, Opportunities and Implimentation," *IEEE,* Vol. 102, No. 1, January 2014.

[3] D. K. C. So, and R. S. Cheng, "Layered maximum likelihood detection for MIMO systems in frequency selective fading channels," *IEEE Trans. on Wireless Communications,* Vol. 5, pp. 752–762, 2006.

[4] G. J. Foschini "Layered Space-Time Architecture for Wireless Communication in a Fading Environment when Using Multi-Element Antennas," *Bell Laboratories Technical Journal,* Vol. 1, No. 2, pp. 41–59, Autumn 1996.

[5] G. J. Foschini, and M. J. Gans, "On the Limits of Wireless Communications in Fading Environment when Using Multiple Antennas," *Wireless Personal Communications,* Vol. 1, No. 3, pp. 311–335, Mar 1998.

[6] G. J. Foschini, G. D. Golden, R. A. Valenzuela, and P. W. Wolniansky, "Simplified Processing for High Spectral Efficiency Wireless Communication Employing Multi-Element Arrays," *IEEE Journal on Selected Areas in Communications,* Vol. 17, pp. 1841–1852, 1999.

[7] Peng Liu, and Shuqing Li, "The Maximum Likelihood Detection for MIMO Communications Systems," *International Conference on E-Product E-Service and E-Entertainment (ICEEE),* Henan, China, pp. 1–3, 2010.

[8] Yavuz Yapici, *V-BLAST/MAP: A New Symbol Detection Algorithm for MIMO Channels,* 2005, The Institute of Engineering and Science of Bilkent University.

[9] Fawaz S. Al-Qahtani, Salama Ikki, Marco Di Renzo, and Hussein Alnuweiri, "Performance Analysis of Space Shift Keying Modulation With Imperfect Estimation in the Presence of Co-Channel Interference," *IEEE Communications Letters,* Vol. 8, pp. 1587–1590, 2014.

[10] P. W. Wolniansky, G. J. Foschini, G. D. Golden, and R. A. Valenzuela, V-BLAST: An Architecture for Realizing Very High Data Rates over the Rich-Scattering Wireless Channel," *Proc. International Symposium on Signals, Systems, and Electronics (ISSSE'98),* Pisa, Italy, Sept–Oct. 1998.

[11] S. M. Alamouti, "A simple transmit diversity technique for wireless communications," *IEEE Journal on Selected Areas in Communications,* Vol. 16, No. 8, pp. 1451–1458, Oct. 1998.

[12] Jeyadeepan Jeganathan et al., "Space Shift Keying Modulation for MIMO Channels," *IEEE,* Vol. 8, pp. 3692–3703, 2009.

[13] V. Tarokh, A. Naguib, N. Seshadri, and A. R. Calderbank, "Combined Array Processing and Space-Time Coding," *IEEE Trans. on Information Theory,* Vol. 45, No. 4, pp. 1121–1128, 1999.

[14] Mehdi Maleki et al., "On the Performance of Spatial Modulation: Optimal Constellation Breakdown," *IEEE Trans. on Communications,* Vol. 62, pp. 144–157, 2013.

[15] R. Mesleh et al., "Spatial Modulation- A New Low Complexity Spectral Efficiency Enhancing Technique," *First International Conference on Communications and Networking in China (ChinaCom'06),* pp. 1–5, 2006.

[16] A. Younis, *Spatial Modulation Theory to Practice,* The University of Edinburgh, 2013.

[17] R. Mesleh and Salama S. Ikki, "A High Spectral Efficiency Spatial Modulation Technique," *IEEE Conf. on Vehicular Technology,* pp. 1–5, Sept 2014.

[18] Jiliang Zhang et al., "Bit Error Probability of Spatial Modulation over Measured Indoor Channels," *IEEE Trans. on Wireless Communications,* Vol. 13, pp. 1380–1387, 2014.

[19] R. Mesleh et al., "Spatial Modulation," *IEEE Trans. on Vehicular Technology,* Vol. 57, No. 4, pp. 2228–2241, July 2008.

[20] Rajab M. Legnain, Roshdy H. M. Hafez, Ian D. Marsland, and Abdelgader M. Legnain, "A novel spatial modulation using MIMO spatial multiplexing," *First international Conf. on Communications, Signal Processing, and their Applications (ICCSPA),* pp. 1-4, 2013.

[21] T. Kailath, H. Vikalo, and B. Hassibi, *MIMO Receive Algorithms.*

[22] Xuehong Cao, "Local Maximum Likelihood Detection Method for MIMO Systems," *Proc. International Conference on Communications, Circuits and Systems,* Vol. 1, pp. 203–206, 2005.

[23] M. Di Renzo, and H. Haas, "Bit Error Probability of Spatial Modulation (SM) MIMO over Generalized Fading Channels," *IEEE Trans. on Vehicular Technology,* Vol. 61, No. 3, pp. 1124–1144, 2012.

[24] M. Di Renzo, and H. Haas, "On Transmit-Diversity for Spatial Modulation MIMO: Impact of Spatial-Constellation Diagram and Shaping Filters at the Transmitter," *IEEE Trans. on Vehicular Technology,* Vol. 62, No. 6, pp. 2507–2531, 2013.

[25] M. D. Renzo, D. D. Leonardis, F. Graziosi, and H. Haas, Space Shift Keying (SSK) MIMO with Practical Channel Estimates, *IEEE Trans. on Communications,* Vol. 60, No. 4, pp. 998–1012, 2012.

[26] M. Di Renzo and H. Haas, Bit Error Probability of Space-Shift Keying MIMO Over Multiple-Access Independent Fading Channels, *IEEE Trans. on Vehicular Technology,* Vol. 60, No. 8, pp. 3694–3711, 2011.

[27] B. Cerato and E. Viterbo, "Hardware Implementation of a Low-Complexity Detector for Large MIMO," *IEEE International Symposium on Circuits and Systems,* pp. 593–596, 2009.

[28] A. Chockalingam, Low-Complexity Algorithms for Large-MIMO Detection, *International Symposium on Communications, Control and Signal Processing (ISCCSP),* pp. 1–6, 2010.

[29] S. Mohammed, A. Chockalingam, and B. Sundar Rajan, A Low-Complexity near-ML Performance Achieving Algorithm for Large MIMO Detection, *IEEE International Symposium on Information Theory,* pp. 2012–2016, 2008.

[30] S. Mohammed, A. Chockalingam, and B. Rajan, High-Rate Space-Time Coded Large MIMO Systems: Low-Complexity Detection and Performance, *IEEE Conf. on Global Telecommunication (GLOBECOM),* pp. 1–5, 2008.

[31] S. Mohammed, A. Zaki, A. Chockalingam, and B. Rajan, High-Rate Space-Time Coded Large-MIMO Systems: Low-Complexity Detection and Channel Estimation, *IEEE Journal of Selected Topics in Signal Processing,* Vol. 3, No. 6, pp. 958–974, 2009.

[32] J. Jeganathan, A. Ghrayeb, and L. Szczecinski, Spatial Modulation: Optimal Detection and Performance Analysis, *IEEE Communication Letters,* Vol. 12, No. 8, pp. 545–547, 2008.

[33] E. Basar, U. Aygolu, E. Panayirci, and H.V. Poor Performance of Spatial Modulation in Presence of Channel Estimation Errors, *IEEE Trans. on Communications,* Vol. 16, No. 2, pp. 176–179, 2012.

[34] Y. Yang, and B. Jiao, Information-Guided Channel-Hopping for High Data Rate Wireless Communication, *IEEE Communication Letters,* Vol. 12, No. 4, pp. 225–227, 2008.

[35] T. Handte, A. Muller, and J. Speidel, BER Analysis and Optimization of Generalized Spatial Modulation in Correlated Fading Channels, *IEEE Conf. on Vehicular Technology,* pp. 1–5, 2009.

[36] Marco Di Renzo, and Harald Hass, Space Shift Keying (SSK) MIMO over Correlated Rician Fading channels: Performance Analysis and a New Method for Transmit-Diversity, *IEEE Trans. on Communications,* Vol. 59, No. 1, pp. 116–129, 2010.

[37] M. Di Renzo, and H. Haas, Bit Error Probability of Space Modulation over Nakagami-m Fading: Asymptotic Analysis, *IEEE Communication Letters,* Vol. 15, No. 10, pp. 1026–1028, 2011.

[38] A. Alshamali, and B. Quza, Performance of Spatial Modulation in Correlated and Uncorrelated Nakagami Fading Channel, *Journal of Communications,* Vol. 4, No. 3, pp. 170–174, 2009.

[39] Salama S. Ikki and Raed Mesleh, A General Framework for Performance Analysis of Space Shift Keying (SSK) Modulation in the Presence of Gaussian Imperfect Estimations, *IEEE Communication Letters,* Vol. 16, No. 2, pp. 228–230, 2012.

[40] M. M. Ulla Faiz, S. Al-Ghadhban and A. Zerguine, Recursive Least Squares Adaptive Channel Estimation for Spatial Modulation Systems, *IEEE Malaysia International Conf. on Communications(MICC),* pp. 785–788, 2009.

[41] Salama S. Ikki, and Sonia Aissa, "Effects of Co-channel Interference on Error Probability Performance of Multi Hop relaying Networks," *IEEE Conf. on Global Telecommunications,* pp. 1–5, 2011.

[42] A. Ribeiro, X. Cai, and G. B. Giannakis, Symbol error probabilities for general cooperative links, *IEEE Trans. on Wireless Communication,* Vol. 4, No. 3, pp. 12641273, May 2005.

[43] J. G. Proakis, *Digital Communications,* 4th ed. Boston: McGraw-Hill, 2001.

[44] A. A. Basri, and T. J. Lim, "Exact Average Bit-Error Probability for Maximal Ratio Combining with Multiple Cochannel Interferers and Rayleigh Fading," *IEEE International Conf. on Communications,* p. 1102–1107, 2007.

[45] Eakkamol Pakdejit,*Linear Precoding Performance of Massive MU-MIMO Downlink System,* 2013, Linkopings University.

[46] E. A. Jorswieck et al., "Performance Analysis of Combining Techniques with Correlated Diversity," *IEEE Wireless Communication and Networking Conference,* Vol. 2, pp. 849–854, 2005.

[47] Kyung Seung Ahn, Robert W. Health Jr., "Performance Analysis of Maximum Ratio Combining with Imperfect Channel Estimation in Presence of Cochannel Interference," *IEEE Trans. on Wireless Communication,* Vol. 8, pp. 1080–1085, 2009.

[48] Reena, Sahasha Namdeo, "Comparative Analysis of Various Diversity Techniques for OFDM Systems," *IOSR-JECE,* Vol. 5, pp. 88–96,2013.

[49] Q. T. Zhang, "Probability of Error for Equal-Gain Combiners Over Rayleigh Channels: Some Closed-form Solutions," *IEEE Trans. on Communications,* Vol. 45, pp. 270–273, 1997.

[50] N. Serafimovski, M. Di Renzo, S. Sinanovic, R. Y. Mesleh, and H. Haas, "Fractional Bit Encoded Spatial Modulation (FBE-SM)," *IEEE Communications Letters* (Vol. 14, No. 5, pp. 429–431, 2010.

[51] Abdelhamid Younis, Nikola Serafimovski, Raed Mesleh, and Harald Haas, "Generalised Spatial Modulation," *Asilomar Conf. on Signals, Systems and Computers* pp. 1498–1502, 2010.

[52] G. Auer at al., "How much Energy is needed to Run a Wireless Network?," *IEEE Wireless Communications,* Vol. 18, No. 5, pp. 40–49, 2011.

[53] C. B. Peel, B. M. Hochwald, and A. L. Swindlehurst, A Vector-Perturbation Technique for Near Capacity Multiantenna Multiuser Communication - Part I: Channel Inversion and Regularization, *IEEE Trans. on Communications,* Vol. 52, No. 1, pp. 195–202, 2005.

[54] J. Jeganathan, A. Ghrayeb, and L. Szczecinski, Generalized Space Shift Keying Modulation for MIMO Channels, *IEEE International Symposium on Personal, Indoor and Mobile Radio Communications,* pp. 1–5, 2008.

[55] M. Di Renzo, and H. Hass, Improving the Performance of Space Shift Keying (SSK) Modulation via Opportunistic Power Allocation, *IEEE Communication Letters,* Vol. 14, No. 6, pp. 500–502, 2010

[56] Z. Wang, and G. B. Giannakis, A simple and general parameterization quantifying performance in fading channels, *IEEE Trans. on Communications,* Vol. 51, No. 8, pp.13891398, Aug. 2003.

[57] Salama S. Ikki, and Sonia Aissa, "Performance Evaluation and Optimization of Dual-Hop Communication over Nakagami-m Fading Channels in the Presence of Co-Channel Interferences," *IEEE Communications Letters* Vol. 16, No. 8, Aug. 2012.

[58] Salama S. Ikki, P. Ubaidulla, and Sonia Aissa, "Performance Study and Optimization of Cooperative Diversity Networks with Co-Channel Interference," *IEEE Trans. on Wireless Communications* Vol. 13, No. 1, Jan. 2014.

[59] Yasir Mehmood et al., "Impact of Massive MIMO Systems on Future M2M Communication," *IEEE Malaysia International Conference on Communications (MICC),* pp. 534–537, 2013.